1. はじめに

日局生物薬品には主に，生物起源由来医薬品，バイオテクノロジー応用医薬品（バイオ医薬品），及び合成ペプチド医薬品が含まれる．日局生物薬品の中心はこれまで，性腺刺激ホルモン類，酵素類及び多糖類などの生物起源由来医薬品であったが，第十六改正第二追補には９品目目の遺伝子組換え医薬品であるインスリングラルギンや，６品目目の合成ペプチドであるリュープロレリン酢酸塩などが収載され，臨床現場での実績を反映して，バイオ医薬品や合成ペプチドの割合が増えてきているといえる．同時に，新規収載医薬品の各条や標準品品質標準では，質量分析（MS），キャピラリー電気泳動，NMR，及び培養細胞を利用した試験法など，既収載品目では利用されていなかった新しい技術が用いられるようになってきている．電気泳動法やペプチドマップ法の改正に向けた国際協力，ヘパリン類の品質・安全性確保及び国際的整合性に向けた各条の継続的な改正，並びに産官学共同による各種試験方法の原案作成も進んでいる．

このように，日局生物薬品の収載状況は，おおむね第十七改正日本薬局方作成の５本の柱である，(1)保健医療上重要な医薬品の全面的収載，(2)最新の学問・技術の積極的導入による質的向上，(3)国際化の推進，(4)必要に応じた速やかな部分改正及び行政によるその円滑な運用，及び(5)日本薬局方改正過程における透明性の確保及び日本薬局方の普及，に添ったものとなっているといえよう．しかし一方で，クオリティ・バイ・デザイン（QbD）により製造・管理された医薬品に対応した記載方針が明確にされていないこと，及び，医療上の重要性や国民の期待が高まっている抗体医薬品の各条収載の目途が立っていないことなど，大きな課題も残されている．本稿では，医薬品各条における生物薬品の収載状況，最新の学問・技術の導入状況，国際調和，及び部分改正状況について，また，QbD で製造・管理された医薬品，及び抗体医薬品各条未収載に対する取り組みについて解説する．

2. 収載状況

第十四改正でインスリンヒトが収載されて以来，遺伝子組換え医薬品原薬として，第十六改正第一追補までに，セルモロイキン及びテセロイキン（インターロイキン-2），エポエチンアルファ及びエポエチンベータ（エリスロポエチン），フィルグラスチム，ナルトグラスチム，及びレノグラスチム（顆粒球コロニー刺激因子類）が収載された（表１）．第十六改正第二追補にインスリングラルギン（インスリンアナログ）が，また，第十七改正以降に，インスリンアスパルト，ソマトロピン，ペグインターフェロンアルファ-2b，及び細胞培養医薬品であるインターフェロンアルファ（NAMALWA）が収載される予定であり，現在，原案審議が続いている．さらに，平成25年12月総合委員会において，エタネルセプト，フォリトロピンベータ，グルカゴンが新規収載候補としてあげられたところである．いずれも1990年代から2000年代前半に承認された品目であり，ソマトロピン，エポエチンアルファ，フィルグラスチム，及びインスリングラルギンのようにバイオ後続品開発の先行品となっている医薬品も含まれている．合成ペプチドでは，エルカトニン，オキシトシン，バソプレシン，カルシトニンサケ，ゴナドレリン酢酸塩に続き，第二追補でリュープロレリン酢酸塩が収載予定である．

3. 最新の学問・技術の導入

生物薬品原薬の品質管理において，HPLC, キャピラリー電気泳動，MS, NMR, SDS-PAGE, 等電点電気泳動，アミノ酸分析，ペプチドマップ法，糖鎖試験，生物活性試験，及びタンパク質定量試験など，様々な分析法や試験方法が用いられるようになってきた．HPLC, MS, NMR, アミノ酸分析は一般試験法として，また，キャピラリー電気泳動，SDS-PAGE, 等電点電気泳動，ペプチド

表1　バイオ医薬品及び合成ペプチド収載状況

	バイオ医薬品	合成ペプチド
第十六改正以前	インスリン ヒト，セルモロイキン，テセロイキン	エルカトニン，オキシトシン，バソプレシン，カルシトニン サケ，ゴナドレリン酢酸塩
第一追補	エポエチン アルファ，エポエチン ベータ，フィルグラスチム，ナルトグラスチム，レノグラスチム	
第二追補	インスリン グラルギン	リュープロレリン酢酸塩
第十七改正以降	インスリン アスパルト，インターフェロン アルファ(NAMALWA)，ペグインターフェロン アルファ-2b，ソマトロピン	
新規候補品	インターフェロン ベータ，フォリトロピン ベータ，エタネルセプト，グルカゴン	合成グルカゴン

（遺伝子組換え）を省略

表2　生物薬品に特徴的な試験方法

	一般試験法	参考情報
第十六改正第二追補以前	アミノ酸分析法	アミノ酸分析法，SDS-PAGE キャピラリー電気泳動，タンパク質定量，等電点電気泳動，ウイルス安全性確保の基本要件，動物由来医薬品起源としての動物に求められる要件，マイコプラズマ否定試験，質量分析，ペプチドマップ法
第十七改正以降（予定）	糖鎖試験法 生物活性試験法	糖鎖試験法（単糖，オリゴ糖） 表面プラズモン共鳴，ELISA

マップ法，タンパク質定量法，マイコプラズマ否定試験，並びに，一般試験法を補完するアミノ酸分析及び質量分析法は参考情報として収載されている（表2）．なお，マイコプラズマ否定試験や後述するペプチドマップ法については改定作業が行われているところである．さらに現在，新規収載に向けて，糖鎖試験法と生物活性試験法の原案作成が進んでいる．

3.1　糖鎖試験法

エリスロポエチン類，リソソーム酵素，抗体，性腺刺激ホルモンはいずれも糖タンパク質であり，糖鎖部分は，活性や体内動態に影響していることが知られている．糖タンパク質医薬品各条では糖鎖試験法が設定されることが多いが，日局では糖鎖試験法が収載されていない．そこで，国立医薬品食品衛生研究所（国立衛研）と生物薬品関連企業は，ヒューマンサイエンス総合事業等の官民共同研究を通じて，糖鎖試験法の作成とその妥当性評価を実施した．糖鎖試験法を構成する単糖，中性オリゴ糖，酸性オリゴ糖，糖ペプチド，及びグリコフォーム分析それぞれの分析法バリデーション結果に基づき作成された糖鎖試験法原案は，日局原案審議委員会生物薬品委員会事務局に提出されたところであり，日局収載に向けた審議が開始される．

3.2　生物活性試験

生物活性試験は，構造が複雑なバイオ医薬品の構造特性の恒常性を包括的に担保する手法として，多くの原薬で設定されている．第十三改正以前から酵素製剤では酵素活性試験が用いられてきたところであるが，遺伝子組換えホルモン類やサイトカイン類の収載に伴い，結合活性や細胞応答

性等を指標とした新しい原理に基づく生物活性試験が導入されるようになってきた．そこで，糖鎖試験と同様に，国立衛研と生物薬品関連企業は共同で，生物活性試験の標準化を行っている．本試験法には表面プラズモン共鳴法，ELISA，細胞応答性試験などが含まれる予定で，表面プラズモン共鳴法はまもなくパブリックコメント収集公開される予定である．ELISA 法も分析法バリデーションを終えたところであり，近日中に ELISA 法原案が生物薬品委員会事務局に提出される予定である．

4. 国際調和

参考情報のうち生物薬品に特徴的な試験，すなわち SDS-PAGE，等電点電気泳動，キャピラリー電気泳動，タンパク質定量法，及びペプチドマップ法は，三局が共同して策定した試験法である．これらは技術の進歩が著しい分析法であり，日局は米国薬局方及び欧州薬局方と共同で既収載試験法の部分改正に取り組んでいる．キャピラリー電気泳動法，及び SDS-PAGE 等についてはすでに改正作業を終え，現在は，ペプチドマップ法の見直しが進んでいるところである．

5. 部分改正状況

生物起源由来医薬品として，消化酵素及び消炎酵素などの酵素類，多糖類，並びに性腺刺激ホルモン類が収載されている．しかし，有害事象発生を食い止められなかった例，実際の製法と試験に不整合が生じている例，及び有効成分を見直すべき例が出始めており，部分改正に向けた対応が行われているところである．

5.1 ヘパリン

2007年，主に米国において，異物混入ヘパリンによる死亡例を含む重篤な有害反応が頻発した．直接的原因は，ヘパリンと同様な抗凝固作用をもつ非天然型多糖類過硫酸化コンドロイチン硫酸（OSCS）が混入されていたことであったが，局方に理化学的試験が採用されていなかったことにより，非天然型異物の混入を防げなかったことも一因と考えられ，日米欧薬局方は協力しながら各条改正を進めてきた．日局でも，2008年一部改正による純度試験 OSCS，第十五改正第二追補による基原の改定，及び2010年一部改正による確認試験の設定，純度試験 OSCS の高感度化，純度試験類縁物質及びガラクトサミンの設定，第十六改正第一追補での純度試験タンパク質及び核酸の追加が行われた（表 3）．さらに，第二追補で，発熱性物質試験からエンドトキシン試験への変更，定量試験の抗 IIa 活性試験への変更及び抗 Xa 活性試験の見直しが予定されている．いずれも，厚生労働省，PMDA，国立衛研及びヘパリン関連企業が協力して対応してきたところであり，第十七改正以降でナトリウム定量を追加することにより，当初の目的が達成されることになる．

しかし，当時，過度に高度な技術として採用されなかった NMR による確認試験が，欧米薬局方では採用されていること，及び，参考情報に核磁気共鳴（NMR）法を利用した定量技術と日本薬局方試薬への応用が収載され，生物学的製剤基準でも多糖類の試験法として採用されている現状を踏まえると，再検討する必要があるかもしれない．また，米国で設定されている分子量分布試験について，日局ではその必要性の議論も開始されていないことなど，まだいくつかの課題は残されていると思われる．

5.2 バソプレシン

バソプレシンとオキシトシンは 9 個のアミノ酸残基からなる下垂体後葉ホルモンであり，現在では合成により供給されている．オキシトシンは基原，及び試験法ともに，実際の製造方法に即した内容に変更され，試験方法も in vivo アッセイから HPLC を用いた理化学的試験に改定されている．これに対して，バソプレシンは，原薬が未収載のまま注射剤が収載されていることもあって部分改正が遅れ，基原に合成または動物由来である

表3　ヘパリンナトリウム部分改正

改正	内容
一部改正 2008.7	純度試験 OSCS の設定
第十五改正第二追補	本品記載の改正
一部改正　2010.1	確認試験，純度試験－ガラクトサミン，純度試験－類縁物質
第十六改正	
第十六第一追補	純度試験－タンパク質，純度試験－核酸，基原の改正
第十六改正第二追補	定量－抗 IIa 活性，示性値－抗 IIa 活性/抗Xa 活性，エンドトキシン
第十七改正以降	定量－ナトリウム塩

ことの記載が残り，後者に対応した純度試験オキシトシンが設定されたままになっている．また，純度試験オキシトシンと，定量法では，試験動物を用いることとされている．第十七改正において，基原の変更と純度試験の見直しが予定されているところであるが，定量試験についても，頑健性，再現性，動物愛護の精神から，理化学的試験への変更を検討しているところである．

5.3　下垂体性性腺刺激ホルモン

下垂体性性腺刺激ホルモンは主に不妊治療に用いられる医薬品であり，有効成分は卵胞刺激ホルモン（FSH）及び黄体形成ホルモン（LH）である．第十六改正では，定量試験として設定されているのは FSH のみであり，LH は純度試験において，LH/FSH が 1 以下であることを確認することとされている．また，FSH 及び LH ともに実験動物による定量試験が採用されているため，頑健性，再現性，動物愛護の精神，また，試験を実施できる機関と試験者の確保が難しいことなどの課題を抱えている．FSH 及び LH は糖タンパク質であることから，理化学的試験法への変更は容易ではないかもしれないが，ELISA などへの変更と，さらには有効成分として LH の含量規格の設定について議論を進めているところである．

6．QbD で製造・管理された医薬品の収載への対応

QbD の考え方は，バイオ医薬品開発初期の頃からすでに取り入れられていた．例えば，アミノ酸配列やウイルス等の安全性の一部は細胞バンクで，また，抗生物質等多くの工程由来不純物は，工程パラメータや工程内管理試験により管理されてきた．しかし，日局各条では，規格及び試験方法によって管理される重要品質特性（CQA）と，その規準しか開示されていない．ICH Q11の調和により，多くの医薬品において管理方法の比重が規格及び試験方法から，原材料，工程パラメータ，工程内管理試験，重要中間体等での管理に移ることが予測される中，各条には記載されない CQA の管理方法を開示する必要性が議論されるようになってきた．そこで，製法で管理される諸問題を議論するために発足した製法問題検討小委員会において，日局生物薬品の製法で管理される CQA に関しては，生物薬品総則や，各条に製造要件の項を設けることにより対応することが提案された．それを受けて生物薬品委員会では，生物薬品総則と製造要件の記載内容について，議論を開始したところである．

7．抗体医薬品収載に向けた対応

リツキシマブ，インフリキシマブ，トラスツズマブは承認されて10年以上が経過した抗体医薬品であり，国内外で高い販売実績と治療実績をあげている．しかし，これらは今後の収載予定品目リストに加わっておらず，保健医療上重要な医薬品の全面的収載を掲げる日局の方針に，どのように応えていくかが課題となっている．

バイオ医薬品は，構造が複雑で不均一であること，また，工程に依存した不純物等が残存し，そ

の許容基準を一律に定めることが困難であることから，異なる製造業者が同一製品を製造・検証することは困難とされている．既承認薬と同等／同質の品質，安全性，有効性を有するものとして異なる製造販売業者により開発される医薬品は，バイオ後続品として扱われる．したがって，ジェネリック医薬品や一般薬が開発される可能性のある化学薬品とは異なり，一部の品目を除く多くのバイオ医薬品の各条収載には，複数の製品の規格の統一という目的はない．各条収載には，国民に品質に関する情報を開示すること，また，規範書として，追随する医薬品の基準・手本となることにより，医薬品全体の品質を向上させるという期待が込められている．抗体医薬品は共通性の高い骨格を持ち，プラットフォーム技術とよばれる類似した製造技術や管理方法を用いた製造・管理が行われる．したがって，個別の品質規格を開示できなくても，抗体医薬品開発と製造において共通して求められる品質要件を，例えば，抗体医薬品各条記載例として示していくことは，抗体医薬品に対する信頼性の確保，及び，新規な抗体医薬品開発と製造の支援，及び品質確保につながるものと考えられる．生物薬品委員会では，抗体医薬品開発支援，品質の向上に資するべく，抗体医薬品の品質要件を明確にするための方策を検討しているところである．

8. さいごに

第十七改正日本薬局方改正の５つの柱に対する取り組みを中心に，日局生物薬品の収載状況と課題を概説してきた．革新的医薬品や次世代バイオ医薬品など開発型研究が推進される中，局方には，既承認薬の品質確保だけでなく，新規医薬品に対して品質管理戦略構築の一般的考え方，標準的管理手法，及び管理基準の目標を提示することの役割も期待されている．日局の新たな役割を見据えて，取り組むべき新たな課題を整理していく必要があるだろう．

謝　辞

本稿は厚生労働科学研究費補助金，及び日局試験法に関する研究（医薬品・医療機器レギュラトリーサイエンス財団）の成果の一部をまとめたものです．また，本稿作成にあたり，生物薬品委員会座長山口照英博士（PMDA/国立衛研），事務局酒井喜代志博士（PMDA 規格基準部）及び高山一成博士（PMDA 規格基準部），並びに委員の先生方にご協力いただきました．特に，糖鎖試験方法の策定，ペプチドマップ法の調和，バソプレシン及び下垂体性性腺刺激ホルモン部分改正について原園景博士（国立衛研），ヘパリンナトリウム各条，生物活性試験の策定及び生物薬品総則について石井明子博士（国立衛研）にご協力いただきました．先生方に心よりお礼申し上げます．

Research Article

Rapid Communications in Mass Spectrometry

Received: 18 July 2013 Revised: 26 January 2014 Accepted: 26 January 2014 Published online in Wiley Online Library

Rapid Commun. Mass Spectrom. **2014**, *28*, 921–932
(wileyonlinelibrary.com) DOI: 10.1002/rcm.6858

Characterization of N-glycan heterogeneities of erythropoietin products by liquid chromatography/mass spectrometry and multivariate analysis

Noritaka Hashii*, Akira Harazono, Ryosuke Kuribayashi, Daisuke Takakura and Nana Kawasaki

Division of Biological Chemistry and Biologicals, National Institute of Health Sciences, 1-18-1 Kamiyoga, Setagaya-ku, Tokyo 158-8501, Japan

RATIONALE: Glycan heterogeneity on recombinant human erythropoietin (rEPO) product is considered to be one of the critical quality attributes, and similarity tests of glycan heterogeneities are required in the manufacturing process changes and developments of biosimilars. A method for differentiating highly complex and diverse glycosylations is needed to evaluate comparability and biosimilarity among rEPO batches and products manufactured by different processes.
METHODS: The glycan heterogeneities of nine rEPO products (four innovator products and five biosimilar products) were distinguished by multivariate analysis (MVA) using the peak area ratios of each glycan to the total peak area of glycans in mass spectra obtained by liquid chromatography/mass spectrometry (LC/MS) of N-glycans from rEPOs.
RESULTS: Principal component analysis (PCA) using glycan profiles obtained by LC/MS proved to be a useful method for differentiating glycan heterogeneities among nine rEPOs. Using PC values as indices, we were able to visualize and digitalize the glycan heterogeneities of each rEPO. The characteristic glycans of each rEPO were also successfully identified by orthogonal partial least-squares discrimination analysis (OPLS-DA), an MVA method, using the glycan profile data.
CONCLUSIONS: PCA values were useful for evaluating the relative differences among the glycan heterogeneities of rEPOs. The characteristic glycans that contributed to the differentiation were also successfully identified by OPLS-DA. PCA and OPLS-DA based on mass spectrometric data are applicable for distinguishing glycan heterogeneities, which are virtually indistinguishable on rEPO products. Copyright © 2014 John Wiley & Sons, Ltd.

Epoetin, recombinant human erythropoietin (rEPO), products are used as erythropoiesis-stimulating agents for renal anemia during dialysis, anemia of prematurity, and cancer-related anemia worldwide. Six innovator products [Epogen (Procrit)/Eprex(Erypo)/Espo (epoetin alfa), NeoRecormon/Epogin (epoetin beta), and Biopoin(Eporatio) (epoetin theta)], and four biosimilar products [Epoetin alfa Hexal (Binocrit)/Abseamed (epoetin alfa), Epoetin alpha BS injection [JCR] (epoetin kappa), and Silapo (Retacrit) (epoetin zeta)] have been marketed in the United States, Japan, and the EU.[1,2]

rEPO is a glycoprotein consisting of 165 amino acid residues with 3 N-glycosylation sites at Asn24, 38, and 83 and an O-glycosylation site at Ser126. Previous reports demonstrated that the main N-glycans of rEPOs are complex-type tetrasialylated tetraantennary glycans. Sialylated fucosyl bi-, tri-, and tetraantennary glycans with and without *N*-acetyllactosamine are also major glycans of rEPOs.[1,3–5] It is well known that the glycosylation of EPO correlates with its biological activity and pharmacokinetics. For example, rEPO with higher sialic acid content, which leads to a longer serum half-life and slower serum clearance, shows low biological activity *in vitro* due to their low affinity for rEPO receptors on the surface of red blood cell precursors.[6–8] It has been suggested that the main chain moieties of N-glycans as well as sialic acids could also be associated with *in vivo* biological activity.[9,10] The heterogeneity of N-glycans on rEPO product is considered to be one of the critical quality attributes, and similarity tests of glycan heterogeneities are required in the manufacturing process changes and developments of biosimilars. Methods that can be used to elucidate highly complex and diverse glycosylation are needed to evaluate comparability and biosimilarity among epoetin batches and products manufactured by different processes.

Glycan analysis has often been performed using liquid chromatography (LC) and capillary electrophoresis (CE) in combination with mass spectrometry (MS).[11–15] These methods are well established and considered as platform technologies for glycan profiling; however, there is a limit to manually distinguish complicated and unclear differences between the glycan heterogeneities of samples when

* *Correspondence to:* N. Hashii, Division of Biological Chemistry and Biologicals, National Institute of Health Sciences, 1-18-1 Kamiyoga, Setagaya-ku, Tokyo 158-8501, Japan.
E-mail: hashii@nihs.go.jp

Copyright © 2014 John Wiley & Sons, Ltd.

significant quantitative and qualitative changes are not observed. Multivariate analysis (MVA) is a predictive method that reduces the number of variables. Interesting differences and characteristics among multiple samples are more easily visualized and understood by MVA.[16] It has been reported that MVA in combination with MS is useful for monitoring impurities of biological products, identifying biomarkers in proteomics, and profiling metabolites in metabolomic studies.[17–19] The MVA method has also been applied to several glycomic approaches and glycan structural analyses for identifying disease-related glycans, clarifying the relationship between disease and glycans, and distinguishing glycan isomers.[20–25]

In this study, the glycan heterogeneities of nine epoetin products were distinguished by MVA using the peak area ratios of glycans in mass spectra obtained by LC/MS using a graphitized carbon column. The differences in glycan heterogeneities among the epeotin products were visualized and digitalized, and the characteristic glycans in each product were identified successfully.

EXPERIMENTAL

1. rEPOs

Four innovator epoetin products, namely Procrit (*epoetin alfa*; Amgen Inc.), Espo (*epoetin alfa*; Kyowa Hakko Kirin Co., Ltd.), Epogin (*epoetin beta*; Chugai Pharmaceutical, Co., Ltd.), and Eprex (*epoetin alfa*; Janssen-Cilag, Ltd.), and five biosimilar products, Epoetin alfa Hexal (*epoetin alfa*; Hexal AG), Binocrit (*epoetin alfa*; Rentschler Biotechnologie GmbH), Silapo (*epoetin zeta*; Standa Arzneimittel AG), Retacrit (*epoetin zeta*; Hospira Inc.), and Epoetin alfa BS injection [JCR] (*epoetin kappa*; JCR Pharmaceuticals Co., Ltd.), were purchased and used in this study as EPO A–I in random order.

2. Preparation of N-glycan samples from rEPOs

Nine commercially available rEPOs obtained from different manufacturers were used in this study. Each rEPO product (100 U) was dissolved in 200 μL of 50 mM sodium phosphate buffer containing 1 mM EDTA (pH 8.0) followed by the addition of 2 U of peptide N-glycosidase F (Roche Diagnostics, Germany). After incubation at 37°C for 16 h, 300 μL of cold ethanol were added to the solution, the mixture was incubated at –20°C for 2 h, and the proteins were removed by centrifugation at 8000*g* at 4°C for 10 min. The supernatants containing N-glycans were evaporated to remove ethanol. The N-glycans were reduced in 500 μL of 0.5 M sodium borohydride at room temperature for 16 h and neutralized with acetic acid. The consequent reduced N-glycans were recovered using a solid-phase extraction cartridge (EnviCarb C, Supelco, Bellefonte, PA, USA), lyophilized, and re-dissolved in 25 μL of ultrapure water as previously described.[11]

3. LC/MS

The analysis of sodium borohydride-reduced N-glycans was performed by liquid chromatography/multiple-stage mass spectrometry (LC/MS^n). The chromatographic separation was performed using an UltiMate 3000 RSLCnano LC system (Dionex, Sunnyvale, CA, USA) with a graphitized carbon column (Hypercarb, 0.1 × 150 mm, 5 μm; Thermo Fisher Scientific, San Jose, CA, USA). The mobile phase was 5 mM ammonium bicarbonate containing 2% acetonitrile (buffer A) and 5 mM ammonium bicarbonate containing 80% acetonitrile (buffer B). The glycans were eluted at a flow rate of 500 nL/min with a linear gradient of 15%–90% buffer B for 60 min. The mass spectra of the reduced N-glycans were acquired using Fourier transform ion cyclotron resonance linear and ion trap type mass spectrometers (FTMS/ITMS, LTQ-FT, Thermo Fisher Scientific) using the software Xcalibur version 2.0 SR2 (Thermo Fisher Scientific). The sequential scan events and analytical conditions were as follows: full mass scan using FTMS (*m/z* 700–2000) and data-dependent MS^n using ITMS; electrospray voltage in negative ion mode, –2.0 kV; capillary temperature, 200°C; tube lens offset, –120 V; collision energy for MS^n (MS/MS, MS/MS/MS, and MS/MS/MS/MS) experiments, 25%; maximum injection times for FTMS and for ITMS, 1250 and 50 ms, respectively; FTMS resolution, 100.

4. MVA

The peak area ratios of each glycan to the total peak area of glycans in mass spectra were used to perform PCA and orthogonal partial least-squares discrimination analysis (OPLS-DA) using the MVA software SIMCA-P+ (Umetrics, Umea, Sweden). The differences between glycan heterogeneities were visualized in the score plot obtained by PCA, and the characteristic glycans of each individual rEPO were found in the loading column plot by OPLS-DA.

RESULTS

1. Characterization of rEPO glycan profiles by PCA score plot

To characterize the glycan heterogeneities of rEPOs by PCA, we first performed glycan profiling of all rEPOs. The sodium borohydride-reduced glycan samples from each rEPO were analyzed by LC/MS^n in the negative ion mode. The glycan structures were deduced on the basis of the accurate mass obtained by high-resolution MS and assignments of fragment ions observed in MS/MS, MS/MS/MS, and MS/MS/MS/MS spectra. As shown in Fig. 1, the total ion current chromatograms (TICCs) of the reduced glycans from the rEPOs excluding EPO-H appeared to be highly similar. By contrast, the TICC of glycans from EPO-H was clearly different from those of the other rEPOs, suggesting that EPO-H possesses noticeable characteristic glycans (as mentioned later). The peak areas of precursor ions corresponding to 57 glycans containing multiple isomers were calculated, and the glycan distribution of each rEPO was drawn on the basis of the peak area ratios of each glycan to the total peak area of all glycans (Fig. 2 and Table 1). Tetrasialylated fucosyl tetraantennary glycan (dHex1 Hex7 HexNAc6 NeuNAc4) was the main glycan in all rEPOs, although there were differences in its content. The major glycans were disialylated fucosyl biantennary glycan (dHex1 Hex5 HexNAc4 NeuNAc2), trisialylated fucosyl triantennary

 Copyright © 2014 John Wiley & Sons, Ltd.

Rapid Communications in Mass Spectrometry

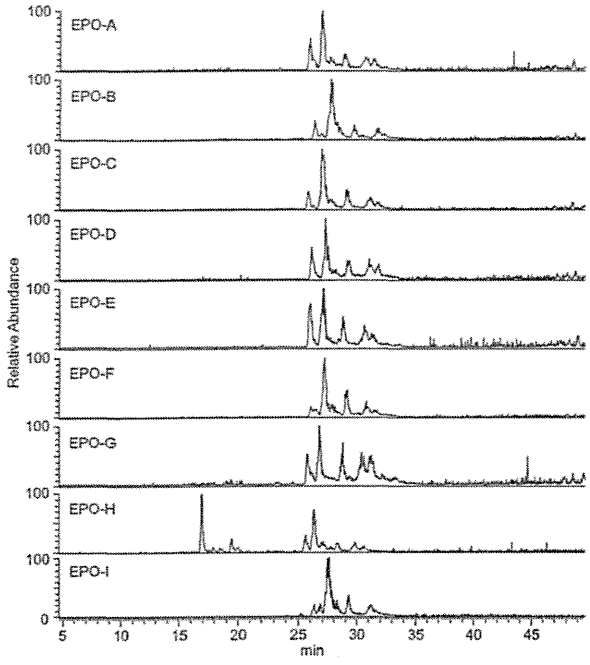

Figure 1. The total ion current chromatograms (base peak chromatograms) of the reduced glycans from rEPOs obtained by LC/MS^n in the negative ion mode.

glycan (dHex1 Hex6 HexNAc5 NeuNAc3), tri- and tetrasialylated fucosyl tetraantennary glycans carrying 1–3 *N*-acetyllactosamine (Lac) motifs (dHex1 Hex8-10 HexNAc7-9 NeuNAc3-4), and tetrasialylated fucosyl tetraantennary glycans carrying 1–2 acetyl groups (dHex1 Hex7 HexNAc6 NeuNAc4 Ac1-2). A high-mannose-type glycan (M6) with 80 Da of additional modification (Hex6 HexNAc2 P1), which is presumed to correspond to phosphorylation, was detected in EPO-B and EPO-C. The complex-type glycans carrying *N*-glycolylneuraminic acid (NeuNGc) were also detected in all rEPOs. Tetrasialylated fucosyl tetraantennary glycans carrying 2–3 Lac motifs (dHex1 Hex9-10 HexNAc8-9 NeuNAc4) and non-fucosylated bi- and triantennary glycans were obvious characteristic glycans of EPO-G and EPO-H, respectively. However, we were unable to identify the discriminative glycans of other EPOs by glycan profiling.

Therefore, next we performed PCA using these peak area ratios. Four principal components were defined by the PCA modeling. Figures 3(A)–3(C) show the score plots for PC1 and PC2, PC1 and PC3, and PC1 and PC4, respectively. These plots allowed us to evaluate the relative similarity in glycan heterogeneities among rEPOs. EPO-A and EPO-H (innovator products) were plotted close to each other in the score plots for PC1 and PC2 (Fig. 3(A)), and for PC1 and PC3 (Fig. 3(B)). EPO-F and EPO-I (innovator products) were also plotted close to each other in the score plots for PC1 and PC2 (Fig. 3(A)), and for PC1 and PC3 (Fig. 3(B)). However, these two groups were differentiated from PC4 (Fig. 3(C)), indicating that these

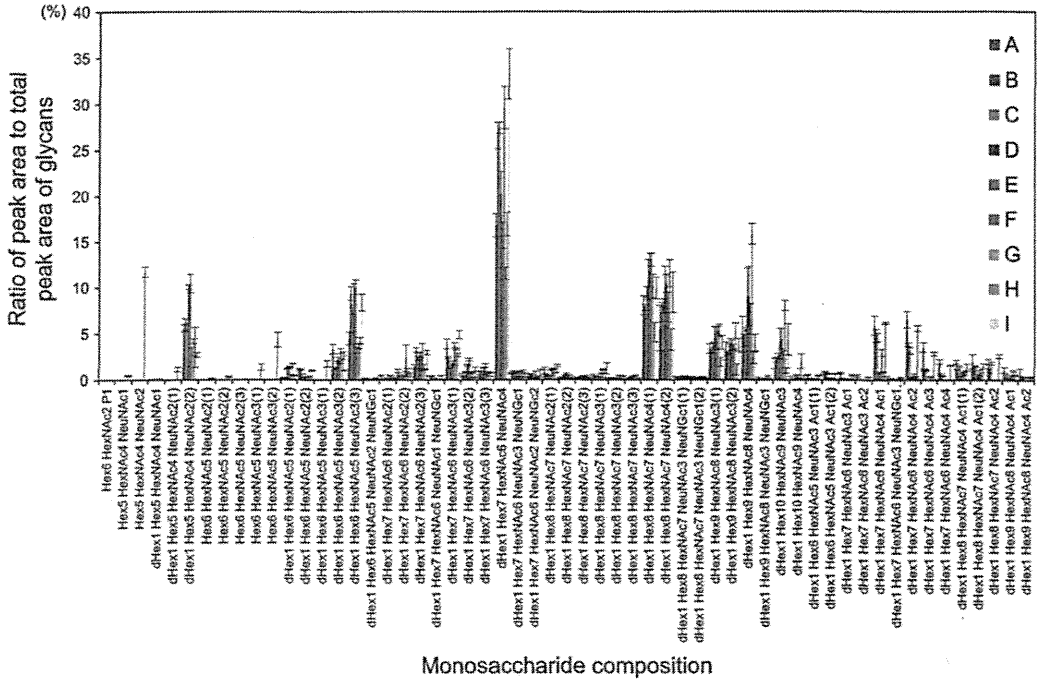

Figure 2. Glycan distributions of EPO-A–I based on the peak area ratios of each glycan to the total peak area of all glycans. An error bar indicates the standard deviation of the peak area ratios obtained from four samples. Hex, hexose; HexNAc, *N*-acetylhexosamine; NeuNAc, *N*-acetylneuraminic acid; NeuNGc, *N*-glycolylneuraminic acid; P, phosphoryl group; Ac, acetyl group.

 Copyright © 2014 John Wiley & Sons, Ltd.

Table 1. Summary of N-glycan profiling from rEPOs

Deduced structure	Monosaccharide composition	Measured *m/z* value	Charge state	Measured accurate mass	Calculated exact mass	Peak area ratio (%) of each glycan to total peak area of glycans from recombinant erythropoietin products								
						A	B	C	D	E	F	G	H	I
M6 P	Hex6 HexNAc2 P1	1477.46	-1	1478.5	1478.5	0.00	0.02	0.02	0.00	0.00	0.00	0.00	0.00	0.00
Bi NeuNAc1	Hex5 HexNAc4 NeuNAc1	965.84	-2	1933.7	1933.7	0.00	0.00	0.00	0.00	0.00	0.00	0.00	0.46	0.00
Bi NeuNAc2	Hex5 HexNAc4 NeuNAc2	1111.38	-2	2224.8	2224.8	0.00	0.00	0.00	0.00	0.00	0.00	0.00	11.72	0.00
Fuc Bi NeuNAc	dHex1 Hex5 HexNAc4 NeuNAc1	1038.87	-2	2079.7	2079.8	0.03	0.08	0.04	0.04	0.05	0.00	0.11	0.06	0.02
Fuc Bi NeuNAc2(1)	dHex1 Hex5 HexNAc4 NeuNAc2(1)	1184.42	-2	2370.8	2370.9	0.00	0.00	0.00	0.00	0.00	0.00	0.00	1.16	0.00
Fuc Bi NeuNAc2(2)	dHex1 Hex5 HexNAc4 NeuNAc2(2)	1184.42	-2	2370.8	2370.9	5.57	5.98	5.63	10.04	10.45	3.08	4.21	3.54	2.72
Tri NeuNAc2(1)	Hex6 HexNAc5 NeuNAc2(1)	1293.96	-2	2589.9	2589.9	0.00	0.00	0.00	0.00	0.00	0.00	0.00	0.20	0.00
Tri NeuNAc2(2)	Hex6 HexNAc5 NeuNAc2(2)	1293.96	-2	2589.9	2589.9	0.00	0.00	0.00	0.00	0.00	0.00	0.00	0.35	0.00
Tri NeuNAc2(3)	Hex6 HexNAc5 NeuNAc2(3)	1293.96	-2	2589.9	2589.9	0.00	0.00	0.00	0.00	0.00	0.00	0.00	0.09	0.00
Tri NeuNAc3(1)	Hex6 HexNAc5 NeuNAc3(1)	1439.50	-2	2881.0	2881.0	0.00	0.00	0.00	0.00	0.00	0.00	0.00	1.39	0.00
Tri NeuNAc3(2)	Hex6 HexNAc5 NeuNAc3(2)	1439.50	-2	2881.0	2881.0	0.00	0.00	0.00	0.00	0.00	0.00	0.00	4.35	0.00
Fuc Tri NeuNAc2(1)	dHex1 Hex6 HexNAc5 NeuNAc2(1)	1366.98	-2	2736.0	2736.0	0.18	0.28	0.13	1.21	1.39	0.54	1.77	0.50	0.48
Fuc Tri NeuNAc2(3)	dHex1 Hex6 HexNAc5 NeuNAc2(2)	1366.98	-2	2736.0	2736.0	1.11	1.18	0.66	0.33	0.38	0.07	0.34	0.07	1.06
Fuc Tri NeuNAc3(1)	dHex1 Hex6 HexNAc5 NeuNAc3(1)	1512.53	-2	3027.1	3027.1	0.00	0.00	0.00	0.00	0.00	0.00	0.00	1.77	0.00
Fuc Tri NeuNAc3(2)	dHex1 Hex6 HexNAc5 NeuNAc3(2)	1512.53	-2	3027.1	3027.1	3.36	1.26	1.23	2.28	1.95	3.15	2.25	2.85	1.07
Fuc Tri NeuNAc3(3)	dHex1 Hex6 HexNAc5 NeuNAc3(3)	1512.53	-2	3027.1	3027.1	4.51	9.35	7.46	9.28	10.05	3.23	3.68	4.27	8.39
Fuc Tri NeuNAc2 NeuNGc1	dHex1 Hex6 HexNAc5 NeuNAc2 NeuNGc1	1520.53	-2	3043.1	3043.1	0.18	0.16	0.10	0.10	0.10	0.08	0.00	0.22	0.08
Fuc Tetra NeuNAc2(1)	dHex1 Hex7 HexNAc6 NeuNAc2(1)	1549.54	-2	3101.1	3101.1	0.49	0.08	0.03	0.15	0.21	0.00	0.48	0.26	0.19
Fuc Tetra NeuNAc2(2)	dHex1 Hex7 HexNAc6 NeuNAc2(2)	1549.54	-2	3101.1	3101.1	1.00	0.42	0.32	0.54	0.44	2.36	1.04	0.73	0.58
Fuc Tetra NeuNAc2(3)	dHex1 Hex7 HexNAc6 NeuNAc2(3)	1549.54	-2	3101.1	3101.1	1.45	3.25	2.32	2.70	2.71	2.45	1.44	1.17	2.97
Fuc Tetra NeuNAc1 NeuNGc1	dHex1 Hex7 HexNAc6 NeuNAc1 NeuNGc1	1557.55	-2	3117.1	3117.1	0.44	0.41	0.18	0.10	0.10	0.08	0.00	0.46	0.10
Fuc Tetra NeuNAc3(1)	dHex1 Hex7 HexNAc6 NeuNAc3(1)	1695.09	-2	3392.2	3392.2	3.91	2.41	1.28	1.67	1.84	3.74	3.36	2.69	4.91
Fuc Tetra NeuNAc3(3)	dHex1 Hex7 HexNAc6 NeuNAc3(2)	1695.09	-2	3392.2	3392.2	0.60	0.29	0.88	1.58	2.22	0.76	0.82	0.27	1.19
Fuc Tetra NeuNAc3(4)	dHex1 Hex7 HexNAc6 NeuNAc3(3)	1695.09	-2	3392.2	3392.2	0.43	0.93	0.62	1.10	1.56	0.58	0.87	0.39	0.78
Fuc Tri NeuNAc4	dHex1 Hex7 HexNAc6 NeuNAc4	1226.76	-3	3683.3	3683.3	16.80	26.58	27.43	20.25	15.71	29.62	11.54	16.92	33.27
Fuc Tri NeuNAc3 NeuNGc1	dHex1 Hex7 HexNAc6 NeuNAc3 NeuNGc1	1232.09	-3	3699.3	3699.3	0.72	0.94	0.77	0.45	0.31	0.86	0.31	0.94	0.67
Fuc Tri NeuNAc2 NeuNGc2	dHex1 Hex7 HexNAc6 NeuNAc2 NeuNGc2	1237.42	-3	3715.3	3715.3	0.28	0.49	0.46	0.40	0.26	0.60	0.21	0.27	0.72
Fuc Tetra Lac NeuNAc2(1)	dHex1 Hex8 HexNAc7 NeuNAc2(1)	1732.11	-2	3466.2	3466.3	1.24	0.64	0.33	0.44	0.44	1.14	1.16	0.77	1.55
Fuc Tetra Lac NeuNAc2(2)	dHex1 Hex8 HexNAc7 NeuNAc2(2)	1732.11	-2	3466.2	3466.3	0.20	0.26	0.26	0.45	0.64	0.22	0.39	0.10	0.27
Fuc Tetra Lac NeuNAc2(3)	dHex1 Hex8 HexNAc7 NeuNAc2(3)	1732.11	-2	3466.2	3466.3	0.10	0.22	0.18	0.34	0.44	0.19	0.44	0.07	0.23
Fuc Tri NeuNAc3(1)	dHex1 Hex8 HexNAc7 NeuNAc3(1)	1877.66	-2	3757.3	3757.3	0.55	0.44	0.36	0.33	0.29	0.70	1.12	0.17	1.26
Fuc Tri NeuNAc3(2)	dHex1 Hex8 HexNAc7 NeuNAc3(2)	1877.66	-2	3757.3	3757.3	0.22	0.06	0.04	0.18	0.23	0.16	0.48	0.12	0.42
Fuc Tri NeuNAc3(3)	dHex1 Hex8 HexNAc7 NeuNAc3(3)	1877.66	-2	3757.3	3757.3	0.14	0.09	0.08	0.27	0.40	0.05	0.50	0.06	0.21
Fuc Tetra Lac NeuNAc4(1)	dHex1 Hex8 HexNAc7 NeuNAc4(1)	1348.47	-3	4048.4	4048.4	8.07	7.83	9.51	10.85	11.88	13.06	10.14	5.16	9.95
Fuc Tetra Lac NeuNAc4(2)	dHex1 Hex8 HexNAc7 NeuNAc4(2)	1348.47	-3	4048.4	4048.4	5.61	7.30	7.99	10.02	10.45	7.87	11.57	4.35	9.48

Copyright © 2014 John Wiley & Sons, Ltd.

Fuc Tetra Lac NeuNAc3 NeuNGc1(1)	dHex1 Hex8 HexNAc7 NeuNAc3 NeuNGc1(1)	1353.81	-3	4064.4	4064.4	0.34	0.26	0.27	0.25	0.27	0.40	0.32	0.32	0.21
Fuc Tetra Lac NeuNAc3 NeuNGc1(2)	dHex1 Hex8 HexNAc7 NeuNAc3 NeuNGc1(2)	1353.81	-3	4064.4	4064.4	0.31	0.22	0.19	0.22	0.18	0.24	0.33	0.27	0.16
Fuc Tetra Lac2 NeuAc3(1)	dHex1 Hex9 HexNAc8 NeuNAc3(1)	1373.14	-3	4122.4	4122.5	3.38	3.16	3.78	4.51	4.60	5.36	5.35	1.95	4.05
Fuc Tetra Lac2 NeuNAc3(2)	dHex1 Hex9 HexNAc8 NeuNAc3(2)	1373.14	-3	4122.4	4122.5	3.13	2.91	3.38	4.05	3.76	3.59	5.32	1.13	3.81
Fuc Tetra Lac2 NeuNAc4	dHex1 Hex9 HexNAc8 NeuNAc4	1470.18	-3	4413.5	4413.6	4.91	4.26	5.43	8.75	9.07	6.57	15.86	2.40	4.03
Fuc Tetra Lac2 NeuNAc3 NeuNGc1	dHex1 Hex9 HexNAc8 NeuNAc3 NeuNGc1	1475.52	-3	4429.6	4429.6	0.19	0.08	0.10	0.10	0.14	0.12	0.38	0.14	0.05
Fuc Tetra Lac3 NeuNAc3	dHex1 Hex10 HexNAc9 NeuNAc3	1494.85	-3	4487.6	4487.6	1.82	2.18	2.54	4.09	4.44	2.67	8.06	1.01	4.39
Fuc Tetra Lac3 NeuNAc4	dHex1 Hex10 HexNAc9 NeuNAc4	1591.89	-3	4778.7	4778.7	0.21	0.08	0.00	0.36	0.34	0.16	2.03	0.00	0.30
Fuc Tri NeuNAc3 Ac1(1)	dHex1 Hex6 HexNAc5 NeuNAc3 Ac1(1)	1533.54	-2	3069.1	3069.1	0.53	0.16	0.13	0.05	0.00	0.17	0.02	0.47	0.00
Fuc Tri NeuNAc3 Ac1(2)	dHex1 Hex6 HexNAc5 NeuNAc3 Ac1(2)	1533.54	-2	3069.1	3069.1	0.72	0.89	0.68	0.16	0.21	0.11	0.03	0.68	0.00
Fuc Tetra NeuNAc3 Ac	dHex1 Hex7 HexNAc6 NeuNAc3 Ac1	1716.10	-2	3434.2	3434.2	0.76	0.15	0.00	0.00	0.00	0.00	0.12	0.52	0.00
Fuc Tetra NeuNAc3 Ac2	dHex1 Hex7 HexNAc6 NeuNAc3 Ac2	1737.10	-2	3476.2	3476.2	0.41	0.00	0.00	0.00	0.00	0.00	0.00	0.31	0.00
Fuc Tri NeuNAc4 Ac	dHex1 Hex7 HexNAc6 NeuNAc4 Ac1	1240.76	-3	3725.3	3725.3	5.90	4.79	4.63	0.79	0.84	2.96	0.89	6.17	0.39
Fuc Tri NeuNAc4 Ac	dHex1 Hex7 HexNAc6 NeuNAc3 NeuNGc1 Ac1	1246.10	-3	3741.3	3741.3	0.16	0.12	0.08	0.00	0.00	0.06	0.00	0.25	0.02
Fuc Tri NeuNAc4 Ac2	dHex1 Hex7 HexNAc6 NeuNAc4 Ac2	1254.77	-3	3767.3	3767.3	6.54	3.83	3.18	0.26	0.25	0.58	0.22	5.58	0.00
Fuc Tri NeuNAc4 Ac3	dHex1 Hex7 HexNAc6 NeuNAc4 Ac3	1268.77	-3	3809.3	3809.3	3.54	1.14	1.06	0.00	0.00	0.37	0.00	2.85	0.00
Fuc Tri NeuNAc4 Ac4	dHex1 Hex7 HexNAc6 NeuNAc4 Ac4	1282.77	-3	3851.3	3851.4	2.00	0.66	0.44	0.00	0.00	0.00	0.00	1.61	0.00
Fuc Tetra Lac NeuNAc4 Ac(1)	dHex1 Hex8 HexNAc7 NeuNAc4 Ac1(1)	1362.47	-3	4090.4	4090.5	1.96	1.16	1.47	0.55	0.57	0.90	0.72	1.42	0.00
Fuc Tetra Lac NeuNAc4 Ac(2)	dHex1 Hex8 HexNAc7 NeuNAc4 Ac1(2)	1362.47	-3	4090.4	4090.5	2.02	1.26	1.51	0.47	0.41	0.76	0.80	1.52	0.00
Fuc Tetra Lac NeuNAc4 Ac2	dHex1 Hex8 HexNAc7 NeuNAc4 Ac2	1376.48	-3	4132.4	4132.5	1.99	1.05	1.83	0.00	0.00	0.00	0.00	2.59	0.00
Fuc Tetra Lac2 NeuNAc4 Ac1	dHex1 Hex9 HexNAc8 NeuNAc4 Ac1	1484.18	-3	4455.5	4455.6	1.12	0.41	0.63	0.30	0.38	0.38	1.03	0.54	0.00
Fuc Tetra Lac2 NeuNAc4 Ac2	dHex1 Hex9 HexNAc8 NeuNAc4 Ac2	1498.19	-3	4497.6	4497.6	0.89	0.27	0.36	0.00	0.00	0.00	0.31	0.38	0.00

dHex, deoxyhexose; Hex, hexose; HexNAc, *N*-acetylhexosamine; NeuNAc, *N*-acetylneuraminic acid; Ac, acetyl group; P, phosphate group; Fuc, fucose; Bi, Tri, and Tetra; bi-, tri-, and tetraantennary complex type glycans; Lac, *N*-acetyllactosamine motif. M6, high-mannose type glycan M6. The number in parentheses indicates isomers.

 Copyright © 2014 John Wiley & Sons, Ltd.

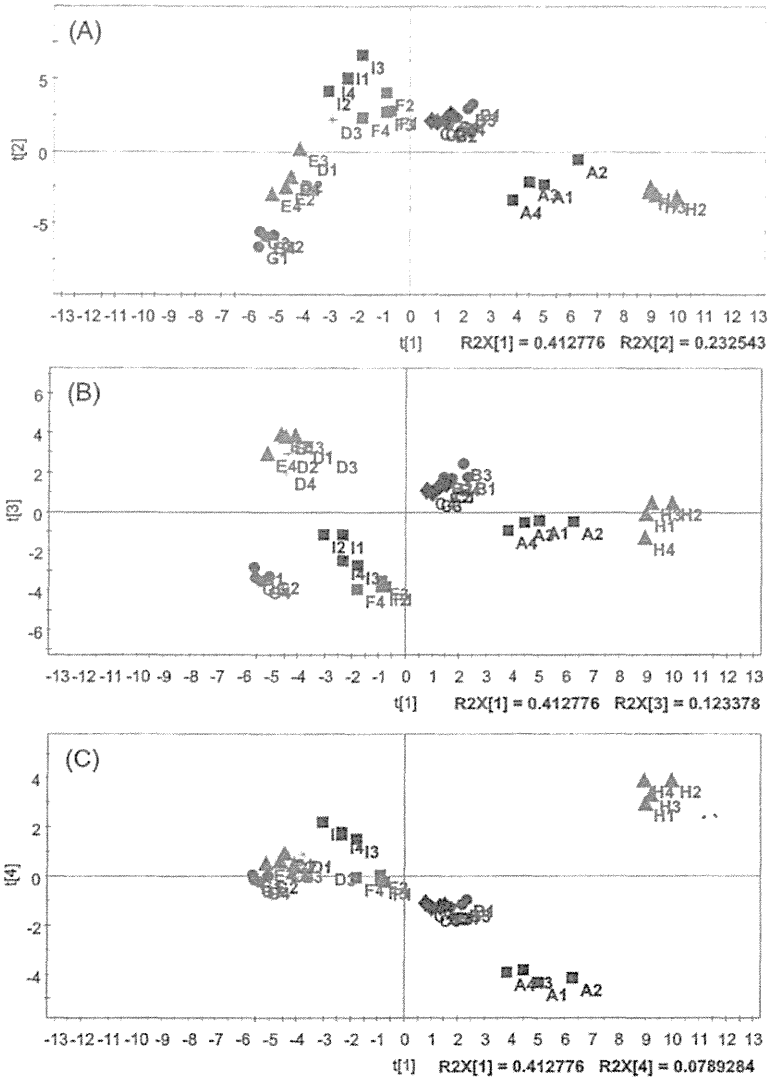

Figure 3. Score plots for PC1 and PC2 (A), PC1 and PC3 (B), and PC1 and PC4 (C) obtained by PCA using the peak area ratios of each glycan to the total peak area of glycans in mass spectra obtained by LC/MS of N-glycans from rEPO products.

rEPOs possess distinctive glycan heterogeneities. EPO-G was located near EPO-D and EPO-E in the score plot for PC1 and PC2 (Fig. 3(A)), and for PC1 and PC4 (Fig. 3(C)), suggesting that the glycan profile of EPO-G is similar to those of EPO-D and EPO-E rather than to those of its reference product (EPO-F). On the contrary, the biosimilar products EPO-B and EPO-C (EPO-B/C), as well as EPO-D and E (EPO-D/E), were plotted close to each other but away from the reference product (EPO-A) in all score plots. This indicated that EPO-B/C and EPO-D/E have similar glycan heterogeneities to each other and different glycan heterogeneities than EPO-A. The PC scores are summarized in Fig. 4. Using the PC values as indices, we were able to digitalize the glycan heterogeneities of each rEPO.

The relative similarities of the glycan heterogeneities among rEPOs were evaluated by hierarchical cluster analysis. Figure 5 shows the dendrogram obtained by cluster analysis. The Euclidean distances between the clusters in the dendrogram were measured by Ward's clustering method. Interestingly, the clusters of EPO-F and EPO-I were classified proximately, suggesting that their glycan heterogeneities were relatively similar. EPO-H was also classified in the neighborhood of the clusters of EPO-A, EPO-B and EPO-C. The relative similarity of the glycan heterogeneities between EPO-B and EPO-C and between EPO-D and EPO-E were re-confirmed.

2. Identification of characteristic glycans by OPLS-DA

PCA is a powerful tool for overviewing the intrinsic variations in a dataset, but it shows a limitation in finding the variables that contribute to the separation among multi-groups because the group information is not reflected in the principal components. OPLS, which is a supervised multivariate projection method providing a maximum separation between groups, is useful in systematically extracting the variables that

 Copyright © 2014 John Wiley & Sons, Ltd.

Rapid Communications in Mass Spectrometry

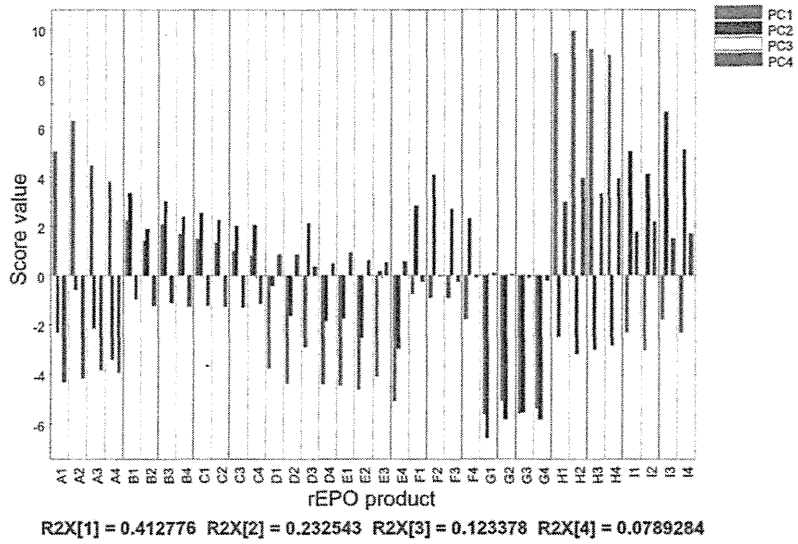

Figure 4. Summary of the PC values obtained by PCA using the peak area ratios of each glycan to the total peak area of glycans in mass spectra obtained by LC/MS of N-glycans from rEPO products.

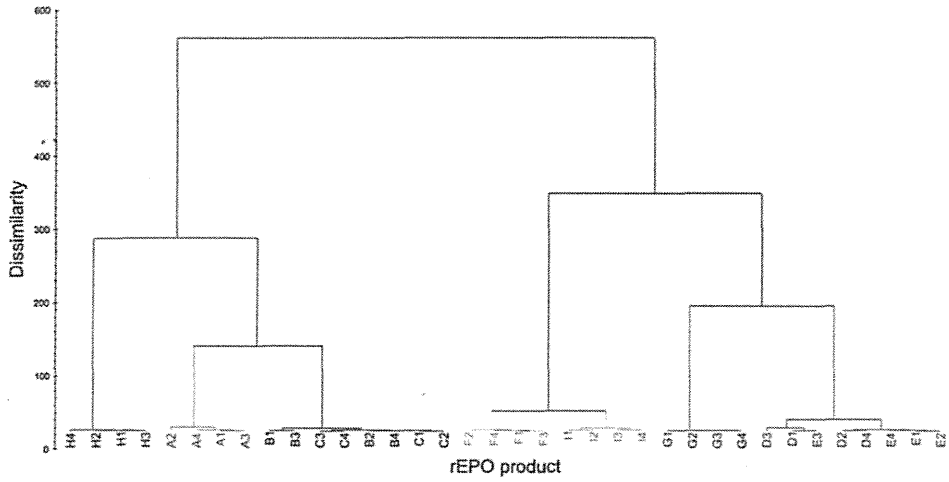

Figure 5. Dendrogram obtained by cluster analysis of the N-glycan distributions of rEPO products. The number of classifications was set as 7.

contribute to the separation among groups. Recently, OPLS-DA has been used to identify biomarker candidates in metabolomics and proteomics.[26,27] We therefore attempted to elucidate the characteristic glycans of each rEPO by OPLS-DA. Figure 6(A) shows the score plot obtained by OPLS-DA between EPO-A and the other rEPOs. The model was composed of a principal component, and the PC values were positive (6.6–7.2). The glycans contributing to the separation between EPO-A and the other rEPOs, i.e., the characteristic glycans of EPO-A, were sorted using the loading column plot (Fig. 7(A)). The glycan with a positive w*[1] value (vertical axis), which is the weight that combines the X variable (the peak area ratio of each glycan), was counted among the characteristic glycans of EPO-A (threshold value >0.1) because the PC values were positive in the score plot (Fig. 6(A)). We considered that the characteristic glycans of EPO-A were tri- and tetrasialylated fucosyl tetraantennary glycans carrying 0–2 Lac motifs and 1–4 acetyl groups as well as some non-acetylated triantennary glycans (Fig. 7(A)). The characteristic glycans of other rEPOs were identified as described for EPO-A (Fig. 7 and Table 2). EPO-B and EPO-D were grouped with EPO-C and EPO-E in consideration of the results of the PCA score plot analyses (Figs. 3–5). The characteristic glycans of EPO-B/C, which are biosimilar products of EPO-A, were di- and trisialylated fucosyl triantennary glycans, trisialylated fucosyl triantennary glycans carrying a acetyl group, di- and tetrasialylated fucosyl tetraantennary glycans, and tetrasialylated fucosyl tetraantennary glycans carrying a Lac motif and 1–2 acetyl groups. The frequency of acetylation of glycans from EPO-B/C was lower than that of EPO-A. In

 Copyright © 2014 John Wiley & Sons, Ltd.

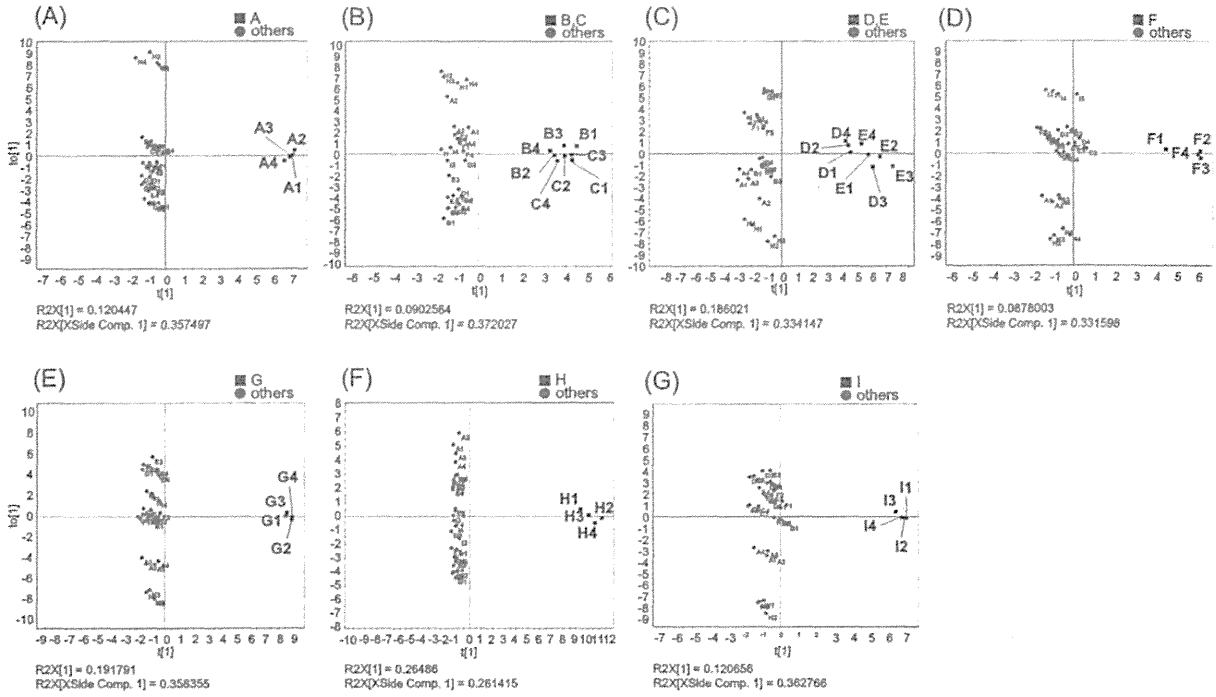

Figure 6. The score plots obtained by OPLS-DA between EPO-A (A), EPO-B and EPO-C (B), EPO-D and EPO-E (C), EPO-F (D), EPO-G (E), EPO-H (F), and EPO-I (H) and other rEPOs.

addition, the deduced phosphorylated M6 was characterized as the discriminative glycan of EPO-B/C, although the w*[1] value was low (0.04). The characteristic glycans of EPO-D/E were disialylated fucosyl biantennary glycans, di- and trisialylated fucosyl triantennary glycans, di- and trisialylated fucosyl tetraantennary glycans, disialylated fucosyl tetraantennary glycan carrying a Lac motif, and tetrasialylated fucosyl tetraantennary glycans carrying 1–2 Lac motifs. The glycans carrying acetyl groups, which are major glycans of EPO-A (the reference product of EPO-D/E), mostly were not detected from EPO-D/E. EPO-F was characterized by a high proportion of highly sialylated glycans, including trisialylated fucosyl triantennary glycans, di- and tetrasialylated fucosyl tetraantennary glycans, and tri- and tetrasialylated fucosyl tetraantennary glycans carrying 1–2 Lac motifs. Interestingly, most of the characteristic glycans of EPO-G were tri- and tetrasialylated fucosyl tetraantennary glycans carrying 1–3 Lac motifs. The characteristic glycans of EPO-H were non-fucosylated bi- and triantennary glycans and tetrasialylated fucosyl tetraantennary glycans carrying acetyl groups. The distinctive glycans of EPO-I were di- and trisialylated fucosyl triantennary glycans, di-, tri-, and tetrasialylated fucosyl tetraantennary glycans, and di, tri-, and tetrasialylated fucosyl tetraantennary glycans carrying a Lac motif, suggesting the certain similarity of glycan heterogeneities between EPO-F and EPO-I.

DISCUSSION

Previous reports of the glycosylation analysis of erythropoietin clarified the diversities and complexities of their acidic N-glycans. For instance, tetrasialylated fucosyl tetraantennary glycans with or without Lac motifs are detected as major glycans from urinary human erythropoietin (hEPO) as well as rEPOs produced in Chinese hamster ovary (CHO) cells, but were not detected in serum hEPO.[28,29] On the contrary, glycans from urinary hEPO and rEPO from CHO cells differ in the linkage position of NeuNAc, i.e., the glycans from urinary hEPO possess NeuNAc(2→3/6) Gal linkages; however, rEPOs possess only NeuNAc(2→3) Gal linkages.[30] Glycosylations of recombinant glycoproteins are affected by manufacturing processes, including the culture conditions as well as cell lines used to express them.[31] Although epoetin alfa and beta are produced in CHO cells and epoetin omega is produced in baby hamster kidney (BHK) cells,[2] it was suggested that the tetrasialylated fucosyl tetraantennary glycan content of epoetin beta was higher than that of epoetin alfa and omega.[29] In addition, the N-glycans of some rEPOs undergo several modifications such as acetylation of NeuNAc and sulfation of non-reducing terminal GlcNAc,[32,33] and high-mannose-type glycan carrying phosphorylated mannose is attached to rEPO from BHK cells and epoetin alfa Hexal, which is a biosimilar of Eprex.[34,35] As previously described, the N-glycan profiles of erythropoietins have been compared among limited erythropoietins in several previous reports; however, the systematic characterizations and discriminations of the glycan heterogeneities between multiple rEPO products were not reported.

In this study, we first characterized the N-glycan heterogeneities of rEPOs by PCA based on the peak area ratios of each glycan to the total peak area of all glycans. The PCA model enabled us to distinguish the glycan

 Copyright © 2014 John Wiley & Sons, Ltd.

Rapid Communications in Mass Spectrometry

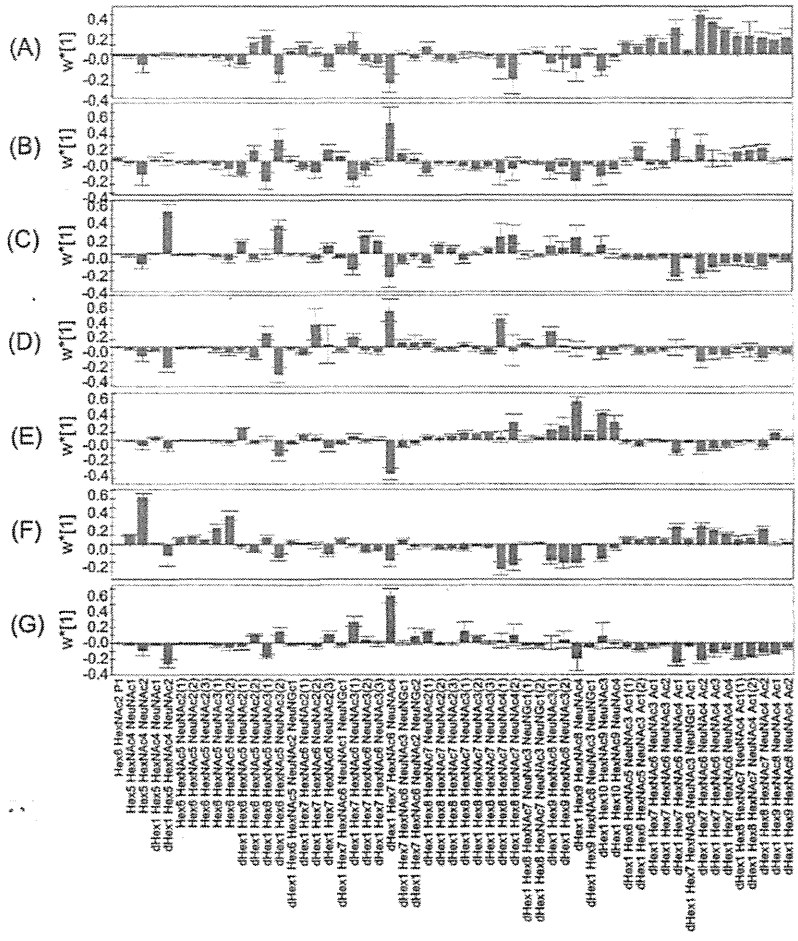

Figure 7. Loading column plots by OPLS-DA between EPO-A (A), EPO-B and EPO-C (B), EPO-D and EPO-E (C), EPO-F (D), EPO-G (E), EPO-H (F), and EPO-I (H) and other rEPOs. The w*[1] value is the weight that combines the X variable. An error bar indicates the standard deviation of w*[1] values obtained from four samples. Hex, hexose; HexNAc, *N*-acetylhexosamine; NeuNAc, *N*-acetylneuraminic acid; NeuNGc, *N*-glycolylneuraminic acid; P, phosphoryl group; Ac, acetyl group.

heterogeneities of four innovator products (EPO-A, EPO-F, EPO-H, and EPO-I) and confirm the similarities of the glycan heterogeneities among the innovator and biosimilar products. Contrary to our expectation, EPO-B/C and EPO-D/E, all of which are biosimilar products of EPO-A, were not plotted near EPO-A, suggesting relative differences between their glycan heterogeneities. We were also able to confirm that the biosimilar product EPO-G is distinguished from its reference product EPO-F. Interestingly, the N-glycan distribution of EPO-G could be similar to that of EPO-D/E rather than EPO-F. As shown in Fig. 4, the visualization and digitalization of the glycan heterogeneities on the basis of the PC values within the PCA model could be useful to objectively evaluate the relative differences of glycan heterogeneities. We next identified the characteristic glycans that contributed to the differentiation of seven rEPO groups in the PCA model by OPLS-DA using the same datasets. The characteristic glycans were different between these groups; in particular, the acetylated glycans, the glycan carrying Lac motifs, and non-fucosylated glycans were distinctive glycans of EPO-A, EPO-G, and EPO-H. Other groups, namely EPO-B/C, EPO-D/E, EPO-F, and EPO-I, display characteristic differences in the number of branches and sialylation of di-, tri-, and tetraantennary glycans. EPO-F and EPO-I exhibited a high proportion of tetrasialylated fucosyl tetraantennary glycans, with EPO-I having a higher proration than EPO-F. By contrast, the major glycans of EPO-D/E were the glycans with lower sialylation and branching. The ratios of the di-, tri-, and tetraantennary glycans of EPO-B/C could be intermediate between those of EPO-D/E, EPO-F, and EPO-I. In addition, the less frequent acetylation of the NeuNAc residues of EPO-D/E, EPO-F, and EPO-I was noteworthy.

 Copyright © 2014 John Wiley & Sons, Ltd.

Table 2. Characteristic glycans of each rEPO

rEPO	Glycan composition	Deduced structure
A	dHex1 Hex6 HexNAc5 NeuNAc2(2)	Fuc Tri NeuNAc2
	dHex1 Hex6 HexNAc5 NeuNAc3(1)	Fuc Tri NeuNAc3
	dHex1 Hex6 HexNAc5 NeuNAc3 Ac1(1),(2)	Fuc Tri NeuNAc3 Ac1
	dHex1 Hex7 HexNAc6 NeuNAc3 Ac1,2	Fuc Tetra NeuNAc3 Ac1-2
	dHex1 Hex7 HexNAc6 NeuNAc4 Ac1-4	Fuc Tetra NeuNAc4 Ac1-4
	dHex1 Hex8 HexNAc7 NeuNAc4 Ac1(1),(2)	Fuc Tetra Lac1 NeuNAc4 Ac1
	dHex1 Hex8 HexNAc7 NeuNAc4 Ac2	Fuc Tetra Lac1 NeuNAc4 Ac2
	dHex1 Hex9 HexNAc8 NeuNAc4 Ac1-2	Fuc Tetra Lac2 NeuNAc4 Ac1-2
B,C	Hex6 HexNAc2 P1	M6-P
	dHex1 Hex6 HexNAc5 NeuNAc2(2)	Fuc Tri NeuNAc2
	dHex1 Hex6 HexNAc5 NeuNAc3(2)	Fuc Tri NeuNAc3
	dHex1 Hex6 HexNAc5 NeuNAc3 Ac1(2)	Fuc Tri NeuNAc3 Ac1
	dHex1 Hex7 HexNAc6 NeuNAc2(3)	Fuc Tetra NeuNAc2
	dHex1 Hex7 HexNAc6 NeuNAc4	Fuc Tetra NeuNAc4
	dHex1 Hex7 HexNAc6 NeuNAc4 Ac1,2	Fuc Tetra NeuNAc4 Ac1-2
	dHex1 Hex8 HexNAc7 NeuNAc4 Ac1(1),(2)	Fuc Tetra Lac1 NeuNAc4 Ac1
	dHex1 Hex8 HexNAc7 NeuNAc4 Ac2	Fuc Tetra Lac1 NeuNAc4 Ac2
D,E	dHex1 Hex5 HexNAc4 NeuNAc2	Fuc Bi NeuNAc2
	dHex1 Hex6 HexNAc5 NeuNAc2(1)	Fuc Tri NeuNAc2
	dHex1 Hex6 HexNAc5 NeuNAc3(2)	Fuc Tri NeuNAc3
	dHex1 Hex7 HexNAc6 NeuNAc2(3)	Fuc Tetra NeuNAc2
	dHex1 Hex7 HexNAc6 NeuNAc3(3)	Fuc Tetra NeuNAc3
	dHex1 Hex8 HexNAc7 NeuNAc2(2),(3)	Fuc Tetra Lac1 NeuNAc2
	dHex1 Hex8 HexNAc7 NeuNAc4(1),(2)	Fuc Tetra Lac1 NeuNAc4
	dHex1 Hex9 HexNAc8 NeuNAc4	Fuc Tetra Lac2 NeuNAc4
F	dHex1 Hex6 HexNAc5 NeuNAc3(1)	Fuc Tri NeuNAc3
	dHex1 Hex7 HexNAc6 NeuNAc2(2)	Fuc Tetra NeuNAc2
	dHex1 Hex7 HexNAc6 NeuNAc4	Fuc Tetra NeuNAc4
	dHex1 Hex8 HexNAc7 NeuNAc4(1)	Fuc Tetra Lac1 NeuNAc4
	dHex1 Hex9 HexNAc8 NeuNAc3(1)	Fuc Tetra Lac2 NeuNAc3
G	dHex1 Hex6 HexNAc5 NeuNAc2(1)	Fuc Tri NeuNAc2
	dHex1 Hex8 HexNAc7 NeuNAc4(2)	Fuc Tetra Lac1 NeuNAc4
	dHex1 Hex9 HexNAc8 NeuNAc3(1),(2)	Fuc Tetra Lac2 NeuNAc3
	dHex1 Hex9 HexNAc8 NeuNAc4	Fuc Tetra Lac2 NeuNAc4
	dHex1 Hex10 HexNAc9 NeuNAc3,4	Fuc Tetra Lac3 NeuNAc3-4
H	Hex5 HexNAc4 NeuNAc1,2	Bi NeuNAc1-2
	Hex6 HexNAc5 NeuNAc3(1),(2)	Tri NeuNAc3
	dHex1 Hex7 HexNAc6 NeuNAc4 Ac1-4	Fuc Tetra NeuNAc4 Ac1-4
	dHex1 Hex8 HexNAc7 NeuNAc4 Ac2	Fuc Tetra Lac1 NeuNAc4 Ac2
I	dHex1 Hex6 HexNAc5 NeuNAc2(2)	Fuc Tri NeuNAc2
	dHex1 Hex6 HexNAc5 NeuNAc3(2)	Fuc Tri NeuNAc3
	dHex1 Hex7 HexNAc6 NeuNAc2(3)	Fuc Tetra NeuNAc2
	dHex1 Hex7 HexNAc6 NeuNAc3(1)	Fuc Tetra NeuNAc3
	dHex1 Hex7 HexNAc6 NeuNAc4	Fuc Tetra NeuNAc4
	dHex1 Hex8 HexNAc7 NeuNAc2(1)	Fuc Tetra Lac1 NeuNAc2
	dHex1 Hex8 HexNAc7 NeuNAc3(1)	Fuc Tetra Lac1 NeuNAc3
	dHex1 Hex8 HexNAc7 NeuNAc4(2)	Fuc Tetra Lac1 NeuNAc4

dHex, deoxyhexose; Hex, hexose; HexNAc, *N*-acetylhexosamine; NeuNAc, *N*-acetylneuraminic acid; Ac, acetyl group; P, phosphate group; Fuc, fucose; Di, biantennary glycan; Tri, triantenarry glycan; Tetra, tetraantennary glycan; Lac, *N*-acetyllactosamine motif. The number in parentheses indicates isomers, which correspond to those in Fig. 2 and Table 1.

It was reported that rEPOs were discriminated on the basis of their glycoforms by PCA using the peak area ratios of intact EPO glycoforms obtained by CE/MS.[4] Whereas the PCA score plot of glycoforms is based on differences in molecular weight, PCA of the released glycan discriminates the many different isomers, as demonstrated in this study. For the differential glycosylation analysis of multiple rEPO products, both glycoform analysis and released glycan analysis could be conducted.

CONCLUSIONS

Discrimination between the glycan heterogeneities of nine rEPO products were performed by MVA using data obtained by LC/MS^n. The PCA values were useful to evaluate the relative differences among the glycan heterogeneities of rEPOs. The characteristic glycans that contributed to the differentiation were also successfully identified by OPLS-DA using the glycan profile data. We demonstrated that

 Copyright © 2014 John Wiley & Sons, Ltd.

PCA and OPLS-DA are applicable for distinguishing glycan heterogeneities that are nearly indistinguishable on rEPO products.

Acknowledgements

This study was supported by a Grant-in-Aid for Scientific Research on Innovative Areas (No. 23110002, Deciphering sugar chain-based signals regulating integrative neuronal functions) from the Ministry of Education, Culture, Sports, Science, Technology (MEXT) of Japan and the Advanced Research for Medical Products Mining Program of the 231 National Institute of Biomedical Innovation (NIBIO) and by a Grant-in-Aid from the Ministry of Health, Labor, and Welfare of Japan.

REFERENCES

[1] A. Harazono, N. Hashii, R. Kuribayashi, S. Nakazawa, N. Kawasaki. Mass spectrometric glycoform profiling of the innovator and biosimilar erythropoietin and darbepoetin by LC/ESI-MS. *J. Pharm. Biomed. Anal.* **2013**, *83*, 65.

[2] J. S. Lee, T. K. Ha, S. J. Lee, G. M. Lee. Current state and perspectives on erythropoietin production. *Appl. Microbiol. Biotechnol.* **2012**, *95*, 1405.

[3] E. Llop, R. Gutierrez-Gallego, J. Segura, J. Mallorqui, J. A. Pascual. Structural analysis of the glycosylation of gene-activated erythropoietin (epoetin delta, Dynepo). *Anal. Biochem.* **2008**, *383*, 243.

[4] A. Taichrib, M. Pioch, C. Neususs. Multivariate statistics for the differentiation of erythropoietin preparations based on intact glycoforms determined by CE-MS. *Anal Bioanal. Chem.* **2012**, *403*, 797.

[5] S. Itoh, N. Kawasaki, M. Ohta, M. Hyuga, S. Hyuga, T. Hayakawa. Simultaneous microanalysis of N-linked oligosaccharides in a glycoprotein using microbore graphitized carbon column liquid chromatography-mass spectrometry. *J. Chromatogr. A* **2002**, *968*, 89.

[6] E. Goldwasser, C. K. Kung, J. Eliason. On the mechanism of erythropoietin-induced differentiation. 13. The role of sialic acid in erythropoietin action. *J. Biol. Chem.* **1974**, *249*, 4202.

[7] S. Elliott, J. Egrie, J. Browne, T. Lorenzini, L. Busse, N. Rogers, I. Ponting. Control of rHuEPO biological activity: the role of carbohydrate. *Exp. Hematol.* **2004**, *32*, 1146.

[8] J. C. Egrie, J. K. Browne. Development and characterization of novel erythropoiesis stimulating protein (NESP). *Br. J. Cancer* **2001**, *84* Suppl 1, 3.

[9] S. Yanagihara, Y. Taniguchi, M. Hosono, E. Yoshioka, R. Ishikawa, Y. Shimada, T. Kadoya, K. Kutsukake. Measurement of sialic acid content is insufficient to assess bioactivity of recombinant human erythropoietin. *Biol. Pharm. Bull.* **2010**, *33*, 1596.

[10] C. T. Yuen, P. L. Storring, R. J. Tiplady, M. Izquierdo, R. Wait, C. K. Gee, P. Gerson, P. Lloyd, J. A. Cremata. Relationships between the N-glycan structures and biological activities of recombinant human erythropoietins produced using different culture conditions and purification procedures. *Br. J. Haematol.* **2003**, *121*, 511.

[11] N. Hashii, N. Kawasaki, S. Itoh, M. Hyuga, T. Kawanishi, T. Hayakawa. Glycomic/glycoproteomic analysis by liquid chromatography/mass spectrometry: analysis of glycan structural alteration in cells. *Proteomics* **2005**, *5*, 4665.

[12] S. Itoh, N. Kawasaki, N. Hashii, A. Harazono, Y. Matsuishi, T. Hayakawa, T. Kawanishi. N-linked oligosaccharide analysis of rat brain Thy-1 by liquid chromatography with graphitized carbon column/ion trap-Fourier transform ion cyclotron resonance mass spectrometry in positive and negative ion modes. *J. Chromatogr. A* **2006**, *1103*, 296.

[13] T. Oyama, M. Yodohsi, A. Yamane, K. Kakehi, T. Hayakawa, S. Suzuki. Rapid and sensitive analyses of glycoprotein-derived oligosaccharides by liquid chromatography and laser-induced fluorometric detection capillary electrophoresis. *J. Chromatogr. B Analyt. Technol. Biomed. Life Sci.* **2011**, *879*, 2928.

[14] M. Pioch, S. C. Bunz, C. Neususs. Capillary electrophoresis/mass spectrometry relevant to pharmaceutical and biotechnological applications. *Electrophoresis* **2012**, *33*, 1517.

[15] M. Pabst, F. Altmann. Glycan analysis by modern instrumental methods. *Proteomics* **2011**, *11*, 631.

[16] G. Ivosev, L. Burton, R. Bonner. Dimensionality reduction and visualization in principal component analysis. *Anal. Chem.* **2008**, *80*, 4933.

[17] K. Laursen, U. Justesen, M. A. Rasmussen. Enhanced monitoring of biopharmaceutical product purity using liquid chromatography-mass spectrometry. *J. Chromatogr. A* **2011**, *1218*, 4340.

[18] J. D. Hu, H. Q. Tang, Q. Zhang, J. Fan, J. Hong, J. Z. Gu, J. L. Chen. Prediction of gastric cancer metastasis through urinary metabolomic investigation using GC/MS. *World J. Gastroenterol.* **2011**, *17*, 727.

[19] K. Kaplan, P. Dwivedi, S. Davidson, Q. Yang, P. Tso, W. Siems, H. H. Hill, Jr. Monitoring dynamic changes in lymph metabolome of fasting and fed rats by electrospray ionization-ion mobility mass spectrometry (ESI-IMMS). *Anal. Chem.* **2009**, *81*, 7944.

[20] T. Chaze, M. C. Slomianny, F. Milliat, G. Tarlet, T. Lefebvre-Darroman, P. Gourmelon, E. Bey, M. Benderitter, J. C. Michalski, O. Guipaud. Alteration of the serum N-glycome of mice locally exposed to high doses of ionizing radiation. *Mol. Cell. Proteomics* **2013**, *12*, 283.

[21] M. M. Gaye, S. J. Valentine, Y. Hu, N. Mirjankar, Z. T. Hammoud, Y. Mechref, B. K. Lavine, D. E. Clemmer. Ion mobility-mass spectrometry analysis of serum N-linked glycans from esophageal adenocarcinoma phenotypes. *J. Proteome Res.* **2012**, *11*, 6102.

[22] E. S. Berman, K. S. Kulp, M. G. Knize, L. Wu, E. J. Nelson, D. O. Nelson, K. J. Wu. Distinguishing monosaccharide stereo- and structural isomers with TOF-SIMS and multivariate statistical analysis. *Anal. Chem.* **2006**, *78*, 6497.

[23] H. B. Oh, F. E. Leach, 3rd, S. Arungundram, K. Al-Mafraji, A. Venot, G. J. Boons, I. J. Amster. Multivariate analysis of electron detachment dissociation and infrared multiphoton dissociation mass spectra of heparan sulfate tetrasaccharides differing only in hexuronic acid stereochemistry. *J. Am. Soc. Mass Spectrom.* **2011**, *22*, 582.

[24] F. E. Leach, 3rd, M. Ly, T. N. Laremore, J. J. Wolff, J. Perlow, R. J. Linhardt, I. J. Amster. Hexuronic acid stereochemistry determination in chondroitin sulfate glycosaminoglycan oligosaccharides by electron detachment dissociation. *J. Am. Soc. Mass Spectrom.* **2012**, *23*, 1488.

[25] Z. T. Hammoud, Y. Mechref, A. Hussein, S. Bekesova, M. Zhang, K. A. Kesler, M. V. Novotny. Comparative glycomic profiling in esophageal adenocarcinoma. *J. Thorac. Cardiovasc. Surg.* **2010**, *139*, 1216.

[26] N. Kaneshiro, Y. Xiang, K. Nagai, M. S. Kurokawa, K. Okamoto, M. Arito, K. Masuko, K. Yudoh, T. Yasuda, N. Suematsu, K. Kimura, T. Kato. Comprehensive analysis of short peptides in sera from patients with IgA nephropathy. *Rapid Commun. Mass Spectrom.* **2009**, *23*, 3720.

[27] H. Tsutsui, T. Maeda, J. Z. Min, S. Inagaki, T. Higashi, Y. Kagawa, T. Toyo'oka. Biomarker discovery in biological specimens (plasma, hair, liver and kidney) of diabetic mice based upon metabolite profiling using ultra-performance

 Copyright © 2014 John Wiley & Sons, Ltd.

liquid chromatography with electrospray ionization time-of-flight mass spectrometry. *Clin. Chim. Acta* **2011**, *412*, 861.
[28] H. Sasaki, B. Bothner, A. Dell, M. Fukuda. Carbohydrate structure of erythropoietin expressed in Chinese hamster ovary cells by a human erythropoietin cDNA. *J. Biol. Chem.* **1987**, *262*, 12059.
[29] V. Skibeli, G. Nissen-Lie, P. Torjesen. Sugar profiling proves that human serum erythropoietin differs from recombinant human erythropoietin. *Blood* **2001**, *98*, 3626.
[30] M. Takeuchi, S. Takasaki, H. Miyazaki, T. Kato, S. Hoshi, N. Kochibe, A. Kobata. Comparative study of the asparagine-linked sugar chains of human erythropoietins purified from urine and the culture medium of recombinant Chinese hamster ovary cells. *J. Biol. Chem.* **1988**, *263*, 3657.
[31] P. L. Storring, R. J. Tiplady, R. E. Gaines Das, B. E. Stenning, A. Lamikanra, B. Rafferty, J. Lee. Epoetin alfa and beta differ in their erythropoietin isoform compositions and biological properties. *Br. J. Haematol.* **1998**, *100*, 79.
[32] N. Kawasaki, M. Ohta, S. Itoh, M. Hyuga, S. Hyuga, T. Hayakawa. Usefulness of sugar mapping by liquid chromatography/mass spectrometry in comparability assessments of glycoprotein products. *Biologicals* **2002**, *30*, 113.
[33] N. Kawasaki, Y. Haishima, M. Ohta, S. Itoh, M. Hyuga, S. Hyuga, T. Hayakawa. Structural analysis of sulfated N-linked oligosaccharides in erythropoietin. *Glycobiology* **2001**, *11*, 1043.
[34] EMA. Epoetin alfa Hexal. *EPAR-Scientific Discussion*, **2007**.
[35] M. Nimtz, V. Wray, A. Rudiger, H. S. Conradt. Identification and structural characterization of a mannose-6-phosphate containing oligomannosidic N-glycan from human erythropoietin secreted by recombinant BHK-21 cells. *FEBS Lett.* **1995**, *365*, 203.

 Copyright © 2014 John Wiley & Sons, Ltd.

JVI
Journals.ASM.org

Separate Cellular Localizations of Human T-Lymphotropic Virus 1 (HTLV-1) Env and Glucose Transporter Type 1 (GLUT1) Are Required for HTLV-1 Env-Mediated Fusion and Infection

Yosuke Maeda,[a] Hiromi Terasawa,[a] Yuetsu Tanaka,[b] Chisho Mitsuura,[a] Kaori Nakashima,[a] Keisuke Yusa,[c] Shinji Harada[a]

Department of Medical Virology, Faculty of Life Sciences, Kumamoto University, Kumamoto, Japan[a]; Department of Immunology, Graduate School of Medicine, University of the Ryukyus, Okinawa, Japan[b]; Division of Biological Chemistry and Biologicals, National Institute of Health Sciences, Tokyo, Japan[c]

ABSTRACT

Interaction of the envelope glycoprotein (Env) of human T-lymphotropic virus 1 (HTLV-1) with the glucose transporter type 1 (GLUT1) expressed in target cells is essential for viral entry. This study found that the expression level of GLUT1 in virus-producing 293T cells was inversely correlated with HTLV-1 Env-mediated fusion activity and infectivity. Chimeric studies between GLUT1 and GLUT3 indicated that the extracellular loop 6 (ECL6) of GLUT1 is important for the inhibition of cell-cell fusion mediated by Env. When GLUT1 was translocated into the plasma membrane from intracellular storage sites by bafilomycin A1 (BFLA1) treatment in 293T cells, HTLV-1 Env-mediated cell fusion and infection also were inhibited without the overexpression of GLUT1, indicating that the localization of GLUT1 in intracellular compartments rather than in the plasma membrane is crucial for the fusion activity of HTLV-1 Env. Immunoprecipitation and laser scanning confocal microscopic analyses indicated that under normal conditions, HTLV-1 Env and GLUT1 do not colocalize or interact. BFLA1 treatment induced this colocalization and interaction, indicating that GLUT1 normally accumulates in intracellular compartments separate from that of Env. Western blot analyses of FLAG-tagged HTLV-1 Env in virus-producing cells and the incorporation of HTLV-1 Env in virus-like particles (VLPs) indicate that the processing of Env is inhibited by either overexpression of GLUT1 or BFLA1 treatment in virus-producing 293T cells. This inhibition probably is due to the interaction of the Env with GLUT1 in intracellular compartments. Taken together, separate intracellular localizations of GLUT1 and HTLV-1 Env are required for the fusion activity and infectivity of HTLV-1 Env.

IMPORTANCE

The deltaretrovirus HTLV-1 is a causative agent of adult T-cell leukemia (ATL) and HTLV-1-associated myelopathy/tropical spastic paraparesis (HAM/TSP). Although HTLV-1 is a complex retrovirus that has accessory genes, no HTLV-1 gene product has yet been shown to regulate its receptor GLUT1 in virus-producing cells. In this study, we found that a large amount of GLUT1 or translocation of GLUT1 to the plasma membrane from intracellular compartments in virus-producing cells enhances the colocalization and interaction of GLUT1 with HTLV-1 Env, leading to the inhibition of cell fusion activity and infectivity. The results of our study suggest that GLUT1 normally accumulates in separate intracellular compartments from Env, which is indeed required for the proper processing of Env.

Human T-lymphotropic virus 1 (HTLV-1) is a complex deltaretrovirus and a causative agent of adult T-cell leukemia (ATL) (62–64) and HTLV-1-associated myelopathy/tropical spastic paraparesis (HAM/TSP) (1, 2). The envelope glycoprotein (Env) of HTLV-1 is synthesized in virus-infected cells as a polyprotein precursor (gp62), which subsequently is cleaved by cellular proteinase(s) localized in the Golgi apparatus into two proteins, surface glycoprotein (gp46; SU) and transmembrane glycoprotein (gp21; TM). HTLV-1 entry is initiated by the specific interaction of SU with cellular receptors, resulting in TM-mediated fusion between viral and cellular membranes.

Three distinct molecules have been shown to be involved in efficient entry of HTLV-1: glucose transporter 1 (GLUT1) (3), heparin sulfate proteoglycans (HSPGs) (4), and neuropilin-1 (NRP-1) (5). It should be noted that transmission of HTLV-1 from virus-infected cells to target cells is mediated mainly by cell-to-cell contact (cell-to-cell infection) (6–8) via virological synapse (9) or biofilm-like extracellular assemblies (10), not by cell-free virus, except in the case of transmission to dendritic cells (11). Although GLUT1 is ubiquitously distributed, HTLV-1 mainly infects human $CD4^+$ T cells (12–15) and immortalizes them (16). In general, the expression of the receptor molecules in target cells is essential for enveloped virus entry. However, surface expression of the receptor molecules in virus-infected cells may interfere with the incorporation of Env or the release of virions because of the association of Env and the receptors. This effect is commonly avoided by simple trapping of the Env-receptor complex in the endoplasmic reticulum (ER) in most viruses. In contrast, another human retrovirus, HIV-1, downregulates or degrades its receptor, CD4, from the plasma membrane of the infected cells by HIV-1

Received 16 September 2014 Accepted 14 October 2014
Accepted manuscript posted online 22 October 2014
Citation Maeda Y, Terasawa H, Tanaka Y, Mitsuura C, Nakashima K, Yusa K, Harada S. 2015. Separate cellular localizations of HTLV-1 Env and GLUT1 are required for HTLV-1 Env-mediated fusion and infection. J Virol 89:502–511. doi:10.1128/JVI.02686-14.
Editor: R. W. Doms
Address correspondence to Yosuke Maeda, ymaeda@kumamoto-u.ac.jp.
Copyright © 2015, American Society for Microbiology. All Rights Reserved.
doi:10.1128/JVI.02686-14

Downloaded from http://jvi.asm.org/ on December 16, 2014 by KUMAMOTO UNIVERSITY

accessory proteins, such as Nef (17–19) and Vpu (20–22), to protect infected cells from superinfection or to maintain the infectivity of HIV-1. However, it remains to be determined how the receptors for HTLV-1, such as GLUT1, are regulated in HTLV-1-infected cells. To address this issue, we overexpressed GLUT1 in virus-producing cells with HTLV-1 Env and checked the cell fusion activity and infectivity. We found that increased expression of GLUT1 in the virus-producing cells inhibited the Env function. Further analyses revealed that GLUT1 is localized in different cellular compartments from Env, resulting in the efficient processing and surface expression of Env in virus-producing cells.

MATERIALS AND METHODS

Cells and culture conditions. The 293T and HeLa cells were cultured in Dulbecco's modified Eagle's medium (DMEM) (Sigma-Aldrich, St. Louis, MO, USA) supplemented with 10% fetal bovine serum (FBS; Gibco BRL, Carlsbad, CA, USA). A human CD4-expressing glioma cell line (NP-2/CD4) (23) and its derivatives (24) were maintained in Eagle's minimum essential medium (MEM; Sigma-Aldrich) supplemented with 10% FBS. The TZM-bl cell line was provided through the AIDS Research and Reference Reagent Program, Division of AIDS, National Institute of Allergy and Infectious Diseases, and maintained in DMEM supplemented with 10% FBS. The Jurkat cell line was purchased from the American Type Culture Collection (ATCC; Manassas, VA, USA) and maintained in RPMI 1640 (Invitrogen, Carlsbad, CA, USA) supplemented with 10% FBS.

Plasmids. An HTLV-1 clone, pMT-2 (25), was provided by M. Matsuoka (Kyoto University). Reporter and packaging plasmids of HTLV-1 and HIV-1 for cell-to-cell infection (6) were kindly provided by D. Derse and G. Heidecker (National Cancer Institute, USA). The plasmids, pNL4-3, pCMV-rev, and pHP-dl-N/A, were obtained through the AIDS Research and Reference Reagent Program, Division of AIDS, National Institute of Allergy and Infectious Diseases. The HIV-1 NL-Luc plasmid pNLLucΔBglII was kindly provided by I. S. Y. Chen (UCSF). A plasmid-enhancing translation initiation, pAdvantage, was purchased from Promega (Madison, WI, USA).

Construction of expression vectors. An expression vector for HTLV-1 Env was constructed from pMT-2 (25). Briefly, the SphI-PstI fragment of pMT-2 carrying HTLV-1 *env* (1.6 kb) was blunt ended and ligated with an EcoRI linker. The *env* fragment digested with EcoRI was further ligated into pcDNA3.1(+) to give pcDNA-1E. The BglII-HindIII fragment carrying the Rev-responsive element (RRE) of pNL4-3 was cloned into pBluescript KS using BamHI and HindIII sites to give pKS-RRE. The XbaI-ApaI fragment of pKS-RRE then was inserted into pcDNA-1E to give pcDNA-1E-RRE. An HTLV-1 Env expression vector with a C-terminal FLAG tag was constructed by using AgeI and XbaI sites of pcDNA-1E-RRE. First, the AgeI-XbaI fragment of the HTLV-1 encoding C-terminal FLAG tag was obtained by PCR using pcDNA-1E-RRE as a template. The primers used were the following: 5′-TTTCCTTGTCACC TGTTCCCAC-3′ and 5′-TCTAGATTACTTGTCGTCATCGTCTTTGT AGTCCAGGGATGACTCAGGGTT-3′ (the underlined portion indicates the XbaI site). The amplified product then was replaced with pcDNA-1E-RRE using AgeI and XbaI sites to give pcDNA-1E-FLAG-RRE. The genes encoding GLUT1 and GLUT3 with C-terminal FLAG tags were cloned by PCR using cDNA libraries of human leukocytes and HeLa cells (Clontech, Mountain View, CA, USA) as the templates, respectively. The primers used were 5′-GCGCTGCCATGGAGCCCAGCAGCAAGAAG-3′ and 5′-GTTACTTGTCGTCATCGTCTTTGTAGTCCACTTGGGAATCAGCC CCCA-3′ for GLUT1 and 5′-CTCGAGGATTACAGCGATGGGGACAC AGAA-3′ and 5′-TTACTTGTCGTCATCGTCTTTGTAGTCGACATTG GTGGTGGTCTCCTT-3′ for GLUT3, and the sequences were verified using a 3130 genetic analyzer (Applied Biosystems, Foster City, CA, USA). Expression vectors for FLAG-tagged GLUT1 and GLUT3 were obtained by the insertion of each fragment into pcDNA3.1(−) using XhoI and HindIII sites for GLUT1 and XhoI and EcoRV sites for GLUT3. Expression vectors for GLUT1 and GLUT3 with C-terminal hemagglutinin (HA) tags were constructed by using StuI and HindIII sites of pcDNA-GLUT1-FLAG and pcDNA-GLUT3-FLAG. The primers used were 5′-CTGCACC TCATAGGCCTCGCTGG-3′ and 5′-AAGCTTAAGCGTAATCTGGAA CATCGTATGGGTACACTTGGGAATCAGC-3′ for GLUT1 and 5′-CA TATGATAGGCCTTGGAGGGATGGC-3′ and 5′-AAGCTTAAGCGTA ATCTGGAACATCGTATGGGTAGACATTGGTGGTGGT-3′ for GLUT3 (underlined portions indicate the StuI and HindIII sites, respectively). The amplified products were replaced with pcDNA-GLUT1-FLAG and pcDNA-GLUT3-FLAG using StuI and HindIII sites to give pcDNA-GLUT1-*HA* and pcDNA-GLUT3-*HA*, respectively. The chimeric expression vectors between GLUT1-FLAG and GLUT3-FLAG first were constructed using common StuI sites located upstream of ECL5 of GLUT1 and GLUT3 genes by swapping restriction fragments. Chimeras between GLUT1 and GLUT3 in ECL5 and ECL6 were constructed with the overlapping extension PCR method as previously described (26). To construct a plasmid encoding GLUT1 with an N-terminal green fluorescent protein (GFP) tag, an XhoI and BamHI fragment of pcDNA-GLUT1-FLAG first was inserted into pEGFP-C1 (Clontech, Mountain View, CA, USA). The FLAG tag was further removed by replacing the SbfI-BamHI fragment of pEGFP-GLUT1-FLAG with the PCR-amplified product using the primers 5′-GACCCATGACCTGCAGGAGATGAAGGAAG-3′ (underlined portion indicates the SbfI site) and 5′-GGATCCTTAAGCCCCCAGGGGAT GGAACAG-3′ (underlined portion indicates the BamHI site) to give pEGFP-GLUT1. An infectious HIV-1 clone lacking the *env* gene (pNL43ΔBglII) was constructed by the deletion of a BglII fragment present in HIV-1 *env*.

Transfection and HTLV-1 Env-mediated cell fusion and infection assay. For the expression of HTLV-1 Env and the production of virus-like particles (VLPs), 293T cells in six-well plates were transfected with 3.5 μg of pNL43ΔBglII, 1.5 μg of pcDNA-1E-RRE, 0.5 μg of pCMV-rev, and 0.5 μg of pAdvantage (Promega) using a Profection kit (Promega) or Lipofectamine 2000 (Invitrogen) according to the manufacturer's recommendations. The expression of GLUT1 in 293T cells was decreased in the indicated experiment by using short interfering RNA (siRNA) against GLUT1 (Sigma) transfected with Lipofectamine 2000 (Invitrogen). The siRNA universal negative control (Sigma) also was used as a negative control. For cell-cell fusion assays, transfected 293T cells were recovered 6 h posttransfection and cocultured with TZM-bl cells. Luciferase activities were measured 30 h posttransfection using a luminometer (Berthold Technology, Bad Wildbad, Germany) as previously described (27). For cell-free infection, luciferase-reporter plasmid pNLLucΔBglII was used instead of pNL43ΔBglII for the transfection. Viral supernatants recovered 24 h posttransfection were used for the infection of NP-2/CD4/CXCR4/CCR5 cells, and luciferase activities of the infected cells were measured 48 h postinfection. The p24 Gag in the culture supernatant was measured using an HIV-1 p24 antigen enzyme-linked immunosorbent assay (Ag ELISA) kit (Zeptometrix, Buffalo, NY, USA) according to the manufacturer's instructions. Cell-to-cell infection assays were performed as previously described (6) using Jurkat cells as the targets. Briefly, 293T cells were cotransfected with pUCHR-inGLucβ, pHP-dl-N/A, pCMV-rev, pAdvantage, and pcDNA-1E-RRE in the presence of pcDNA-GLUT1-FLAG, pcDNA-GLUT3-FLAG, or empty vector. Transfected cells were recovered 6 h posttransfection and cocultured with Jurkat cells. The luciferase activities were measured after 48 h of coculture.

Flow cytometry. The 293T cells were transfected with pcDNA-GLUT1-FLAG, pcDNA-1E-RRE, pNL43ΔBglII, pCMV-rev, and pAdvantage as described above. The cells were recovered 24 h posttransfection using cell dissociation solution (Sigma) and stained with anti-gp46 rat monoclonal antibody (MAb) LAT-27 (28), followed by staining with allophycocyanin (APC)-conjugated anti-rat IgG (BioLegend, San Diego, CA, USA). The cells were further stained with fluorescein isothiocyanate (FITC)-conjugated anti-GLUT1 (R&D Systems, Minneapolis, MN, USA), fixed with 4% paraformaldehyde for 15 min, and analyzed using a

Downloaded from http://jvi.asm.org/ on December 16, 2014 by KUMAMOTO UNIVERSITY

FACSCalibur fluorescent-activated cell sorter (BD Biosciences, San Jose, CA, USA).

Laser scanning confocal microscopy. The HeLa cells were plated on poly-L-lysine-coated eight-well glass slides (Matsunami Glass, Osaka, Japan), transfected with pEGFP-GLUT1 and pcDNA-1E-RRE using Lipofectamine 2000 (Invitrogen) according to the manufacturer's instructions, and cultured for 24 h. The cells were fixed with 4% paraformaldehyde for 15 min. The fixed cells were permeabilized with 0.2% Triton X-100 and stained with the anti-gp46 rat MAb LAT-27 (28), stained with anti-rat IgG conjugated with Cy3 (Jackson ImmunoResearch), and analyzed using an LSM-700-Zen confocal laser scanning microscope (Carl Zeiss, Gottingen, Germany) with a 60× objective lens. The images were processed using the LSM imaging browser (Carl Zeiss).

Immunoprecipitation and Western blotting. The 293T cells in six-well plates were transfected with 3.5 μg of pNL43ΔBglII, 1.5 μg of pcDNA-1E-RRE, 0.5 μg of pCMV-rev, and 0.5 μg of pAdvantage (Promega) using Lipofectamine 2000 (Invitrogen) and then cultured for 24 h at 37°C. The cells then were solubilized using 1% Brij O10 (Sigma-Aldrich) lysis buffer (1% Briji O10, 20 mM Tris-Cl, pH 8.0, 150 mM NaCl) with a protease inhibitor cocktail (Nakalai Tesque, Kyoto, Japan). For the preparation of VLPs, culture supernatants from transfected 293T cells were harvested after 24 h of culture and filtered through 0.45-μm-pore-size filters. The filtered supernatants then were centrifuged at 10,000 × *g* for 1 h at 4°C. The pellets were resuspended in 2× loading buffer. The cell lysates or VLPs then were separated by SDS-PAGE and blotted onto PVDF (polyvinylidene difluoride; Immobilon-P; Millipore, Billerica, MA, USA) membranes. The membranes were incubated with anti-gp46 rat MAb (LAT-27), anti-FLAG mouse MAb (Wako, Osaka, Japan), anti-HA mouse MAb (Wako), anti-HIV-1 Gag mouse MAb (24-3) (29), anti-cyclophilin A (CypA) rabbit polyclonal antibody (Enzo Life Sciences, Farmingdale, NY, USA), or anti-β-actin mouse MAb (Sigma), followed by staining with horseradish peroxidase (HRP)-conjugated anti-mouse (Jackson ImmunoResearch, West Grove, PA, USA), anti-rat (Jackson ImmunoResearch), or anti-rabbit (Jackson ImmunoResearch) IgG. The signals were detected using Chemi-Lumi One (Nacalai Tesque). For immunoprecipitation, the cells first were treated with DSP (dithiobis[succinimidylpropionate]) cross-linker according to the manufacturer's instructions (Thermo Scientific, Rockford, IL, USA) and solubilized using 1% Brij O10 lysis buffer with a protease inhibitor cocktail. Cell lysates were incubated with anti-FLAG mouse MAb (Wako) for 1 h at 4°C. Sepharose-protein G beads (GE Healthcare Life Sciences, Uppsala, Sweden) were added, and samples were incubated overnight at 4°C. Samples were washed four times with 1% Brij O10 lysis buffer, resuspended in 2× loading buffer, and subjected to SDS-PAGE. Proteins were analyzed by Western blotting using anti-gp46 rat MAb (LAT-27). The reactions also were enhanced by using Can Get signal (Toyobo, Osaka, Japan).

RESULTS

Inhibition of HTLV-1 Env-mediated cell fusion and infection by overexpression of GLUT1 in VLP-producing 293T cells. It has been shown that the expression of GLUT1 in target cells is essential for entry for HTLV-1 (3). However, it is unknown whether the expression of GLUT1 in virus-producing cells affects the efficiency of virus entry, because GLUT1 is physically associated with HTLV-1 Env (3). To address this issue, we selected 293T cells as VLP-producing cells, because 293T cells typically express low levels of GLUT1 on their cell surfaces (Fig. 1A). For the efficient production of VLPs, HIV-1 vectors pseudotyped with HTLV-1 Env also were used in this study. The overexpression of FLAG-tagged GLUT1 in VLP-producing cells, which was confirmed by Western blotting (Fig. 1B), increased the surface expression level of GLUT1 (Fig. 1A). GLUT1 also was preferentially incorporated into VLPs during the overexpression of GLUT1 compared with the level during overexpression of GLUT3, irrespective of the expression of HTLV-1 Env (Fig. 1B). When GLUT1 and HTLV-1 Env were coexpressed in VLP-producing 293T cells, the surface expression level of gp46 did not appear to be affected by overexpression of GLUT1 compared with the expression level in mock-transfected 293T cells (Fig. 1B).

We also noticed that mature gp46 was not incorporated into VLPs produced from 293T cells expressing large amounts of GLUT1. The larger molecular size recognized by anti-gp46 in VLPs (~53 kDa), which corresponds to the size of an underglycosylated and uncleaved form of Env, most likely was due to the contamination of intracellular materials of the cells. In contrast, mature gp46 was incorporated into the VLPs produced from mock- or GLUT3-transfected 293T cells (Fig. 1B). The cell-cell fusion activity, cell-to-cell infectivity, and cell-free virus infectivity also were profoundly reduced by the overexpression of GLUT1 but not by the overexpression of GLUT3 in VLP-producing 293T cells (Fig. 1C). In contrast, fusion activity and infectivity mediated by HIV-1 Env, including cell-cell fusion, cell-to-cell infection, and cell-free infection, were not inhibited by overexpression of GLUT1 or GLUT3 (data not shown). To exclude the effect of VLPs produced by HIV-1 vectors, we also checked the effect of VLPs produced by HTLV-1 vectors. We found that overexpression of GLUT1 in HTLV-1-VLP-producing cells also specifically and profoundly inhibited HTLV-1 Env-mediated cell-to-cell infection (Fig. 1D). These results indicate that GLUT1 specifically inhibits HTLV-1 Env-mediated cell fusion and infectivity, probably owing to the loss of mature gp46 incorporation into VLPs.

Inverse correlation between the expression level of GLUT1 and the fusion activity of HTLV-1 Env in VLP-producing 293T cells. We further checked whether the expression level of GLUT1 is correlated with the inhibition of HTLV-1 Env-mediated fusion. When 293T cells were transfected with increasing amounts of the plasmid encoding FLAG-tagged GLUT1, GLUT1 was increasingly incorporated into VLPs (Fig. 2A), while HTLV-1 Env-mediated fusion activity and infectivity were inversely inhibited (Fig. 2B) in a dose-dependent manner.

We next sought to check whether the knockdown of GLUT1 in VLP-producing 293T cells augments the infectivity of HTLV-1 Env-bearing VLPs, because 293T cells still endogenously express a low level of GLUT1. The knockdown of GLUT1 by siRNA first was verified by an observed reduction of FLAG-tagged GLUT1 expression (Fig. 2C), because the endogenous level of GLUT1 in 293T cells was undetectable using anti-GLUT1 antibodies in Western blotting (data not shown). We found that cell-free virus infectivity recovered from VLP-producing 293T cells cotransfected with siRNA against GLUT1 was significantly increased compared with the infectivity of virus recovered from cells transfected with negative-control siRNA (Fig. 2C). These results indicate that the fusion activity of HTLV-1 Env is inversely related to the expression level of GLUT1 in VLP-producing cells.

The ECL6 region of GLUT1 is sufficient for the inhibitory activity of GLUT1 against HTLV-1 Env-mediated fusion. Because GLUT3, which shares 63% amino acid sequence identity with GLUT1, had no inhibitory effect on HTLV-1 Env-mediated cell fusion, as shown in Fig. 1, we sought to determine the region of GLUT1 responsible for inhibition of HTLV-1 Env cell fusion activity. Using a common restriction site and overlapping extension PCR methods, we generated a series of GLUT1-GLUT3 chimeras, as shown in Fig. 3A. The inhibitory activity against cell fusion for

Downloaded from http://jvi.asm.org/ on December 16, 2014 by KUMAMOTO UNIVERSITY